Examining the capabilities of SWOT to derive the tidal characteristics in the North Sea

by

Bram Pleij

Master's thesis

Department of Physical Geography

Faculty of Geosciences

Utrecht University

July 2025

Contents

Summary

The Surface Water and Ocean Topography (SWOT) satellite provides a promising new method to measure the global sea surface height (SSH). With the use of radar interferometry, it is possible to improve the spatial resolution by an order of magnitude compared to previous missions using radar altimetry. This development can help with the understanding of mesoscale and submesoscale oceanic processes. Additionally, tidal reconstruction based on observations in challenging environments, such as high latitude and coastal areas, can benefit. However, the accuracy of SWOT in challenging environments, such as the Dutch coastal zone has not yet been fully tested. Using in-situ measurements of tidal gauge stations of Rijkswaterstaat (RWS), the SSH measurements of the SWOT_L2_LR_SSH_EXPERT_2.0 dataset are validated. Here it is shown that the correlation between SWOT and tidal gauge data is good (R^2 = 0.88, RMSE = 0.22m). However, the quality of the SWOT measurements decreases towards the coast (6.3% 'good quality' data points, compared to 48% further from the coast). In the Wadden Sea the correlation decreases to 0.79, with a RMSE of 0.34m and only 0.79% 'good quality' datapoints. Additionally, the possibility of using SWOT data to reconstruct the tidal signal over a large area has not yet been fully explored. In this paper a new approach to reconstruct the tidal signal using a representative tidal cycle based on SWOT data has been tested successfully. The M_2 tidal constituent showed a good fit (high SNR). However, the M_4 tidal constituent was less accurate, likely because the amplitude (0-0.3m) is in the same range as the error in SSH measurements. Although it lacks in the possibility to resolve low resolution tidal constituents, it is able to fit the dominant semidiurnal tidal component in the North Sea. The demonstrated approach can be useful for further studies that want to reconstruct the tidal signal with limited temporal data availability.

1. Introduction

Ocean tides play a crucial role in a variety of oceanic processes, including coastal dynamics and ocean mixing (Hart-Davis et al., 2021). Understanding tides is also relevant for studies that focus on non-tidal signals. For example, in sea-level rise and ocean circulation research, the tidal component must be accurately removed to isolate long-term trends. Over recent decades, data-assimilative global tide models have significantly improved, largely due to advances in observational data used for validation of the models (Stammer et al., 2014). Stammer found a root-mean-square (RMS) difference of M_2 tide models relative to pelagic bottom pressure stations of 0.51 cm, this is a strong improvement compared to the previously reported difference of 1.64 cm by Shum et al. in 1997. This model improvement can be explained for about half with improvements in the test data. This example shows that improvements in sea surface height (SSH) measurements, which the tidal models use as test data, can benefit the accuracy of such models. The expansion of tidal gauge networks has enhanced in-situ measurements, while satellite altimetry has provided more extensive and precise data over the global ocean (Stammer et al., 2014). Together, these developments contribute to a more detailed and reliable picture of tidal dynamics. Furthermore, there are differences in the accuracy of tidal modelling in different environments. Stammer showed that the RMS values in pelagic conditions (0.89 cm) are substantially lower than in shelf and coastal conditions (5.1 cm and 6.5 cm respectively). In shallow waters, short scale tidal components, such as the M_4 constituent, are harder to detect using traditional satellite altimetry with a small resolution. An overview of previous satellite altimetry missions with their spatial resolution is given in section 1.1, Table 1. The Surface Water and Ocean Topography (SWOT) mission can provide the next step for global, high-resolution measurements of the water level. The high spatial resolution is able to capture small-scale tidal features, improving the accuracy of SSH measurements in shelf seas, ultimately improving the quality of test data used in assimilative tide models. In this thesis, SWOT satellite data is combined with tidal gauge measurements to assess the improvements in SSH measurements. The primary aim is to highlight the advancements offered by SWOT compared to earlier SSH surveys using conventional satellite altimetry. To provide context, the following section outlines the key developments in SSH measurement techniques leading up to the introduction of radar interferometry, used by SWOT.

1.1 Advances in sea surface heigh observation

Modern sea-level measuring began in the nineteenth century with the development of the first self-recording tide gauge (Matthäus, 1972). From this moment, a network of tide gauges gradually spread around the world, providing measurements on the water level. Technical developments and the establishment of a global network of tide gauges have enabled long-term, consistent observations of sea level and tides across much of the world's waters. To understand the tidal signal, generally a set of harmonic constituents is fit to the data (Intergovernmental Oceanographic Commission, 2006). For harmonic analysis the tidal signal is broken down into multiple components with specific frequencies and amplitudes. This gives a good understanding of tidal behaviour. However, the spatial distribution of tides is still a problem. Tidal gauges offer long time series, but only at fixed locations. As a result, large regions of the global ocean, particularly offshore and in the polar regions, remain undersampled (e.g. Ray, 2013; Stammer et al., 2014). These in-situ measurements form the foundation of tidal analysis, sea-level trend estimation, and the validation of satellite altimetry data (Merrifield et al., 2009). Satellite altimetry represents a major advancement in SSH measurements by overcoming the key limitation of tide gauges, namely their uneven spatial distribution. The arrival of satellite altimetry has been able to provide a global, high-resolution image of the sea level. This solved the bias of tidal gauges towards coastal and populated areas. Since the launch of the first satellite with an altimeter on board in the 1970's (Pugh, 1987), satellite altimetry has advanced significantly. Table 1 presents an

overview of the most relevant missions and their key characteristics. The vertical accuracy of SSH measurements depends primarily on two factors: the precisions of the altimeter's range measurements and the accuracy of the satellite's orbit determination. The improvement in orbit determination has contributed most significantly to the overall accuracy. This had been made possible by the integration of precise tracking systems, such as Satellite Laser Ranging (SLR), DORIS (Doppler Orbitography and Radiopositioning Integrated by Satellite), and onboard GPS receivers (Fu & Cazenave, 2000). The TOPEX/Poseidon mission was the first to incorporate these technologies, greatly reducing uncertainty in altimetric measurements. Together with the Jason series it has established a long-term, high-accuracy sea level record.

SATELLITE	YEARS ACTIVE	REVISIT TIME	ORBIT ACCURACY	RANGE PRECISION	SPATIAL RESOLUTION	INCLINATION
SEASAT	1978	~17 days	~1 m	~20 cm	~1.5°	108°
GEOSAT	1985–1989	17 days	~50 cm	~20 cm	~0.5°	108°
TOPEX/POSEIDON	1992–2006	10 days	~2–3 cm	~2 cm	~0.25°	66°
JASON-1/2/3	2001–2023	10 days	~2–3 cm	~2–3 cm	~0.25°	66°
SENTINEL-3A/B	2016–present	27 days	~2–3 cm	~2–3 cm	~0.3°	98.6°
SWOT	2022–present	21 days	~1–2 cm	~2 cm	~0.05°	77.6°

Table 1: Description of main characteristics of relevant past and current satellite altimetry missions.

The SWOT satellite builds on traditional satellite altimetry by introducing an advanced measurement technique, radar interferometry. This technique made it possible to significantly reduce the spatial resolution of satellite derived SSH measurements (Table 1).

1.2 Satellite altimetry and radar interferometry

To have a better understanding of the SWOT satellite and the SSH measurements it provides it is important to know the principles behind it. It is essential to first understand the principles and limitations of conventional altimetry before discussing the methodology used by SWOT. Satellite altimetry measures the distance between a satellite and the sea surface by transmitting a short pulse of microwave radiation at high frequency and recording the time delay of its return signal (Chelton et al., 2001). The time measurement is scaled to the speed of light, which returns the uncorrected range (Figure 1). However, a number of corrections need to be applied which are related to atmospheric refraction and biases due to the sea state.

Atmoshperic refraction causes the electromagnetic wave to have a longer travel time when travelling through the atmosphere. The atmospheric refraction is determined by the temperature, pressure, water vapour density, cloud liquid water droplet density, presence of raindrops and ionospheric electron density. It is difficult to quantify the effects of rain on the range estimates, so altimeter observations who are likely to be affected by rain are flagged. To know the different parameters that

effect the atmospheric refraction, satellites with altimeters need to also measure these atmospheric conditions. Although a weather model can also be used for determining atmospheric corrections.

The sea state creates biases in the altimeter measurements as well. The form of the waves is the main reason for these biases. The electromagnetic bias is a result of a difference in the reflection rate between the wave troughs and the wave crests. Wave troughs are flattened and hence have a higher reflection rate compared to the wave crests. Additionally, wind generated small-scale roughness of the sea surface is greater near wave crests than in wave troughs, reducing the reflectance of the radar signal. The signal reflected from wave troughs is thus greater than from wave crests, which causes the average point of reflection to be slightly below the actual mean sea level and thus gives an underestimation of the sea level. The skewness bias is a result of the height difference between the mean scattering surface and the median scattering surface. The mean scattering surface is the average of the heights of the wave crests and the wave troughs. The median scattering surface is what is actually measured by the altimeter, the half-power point of the return signal. This results in an underestimation of the water surface level (Volkov, 2004).

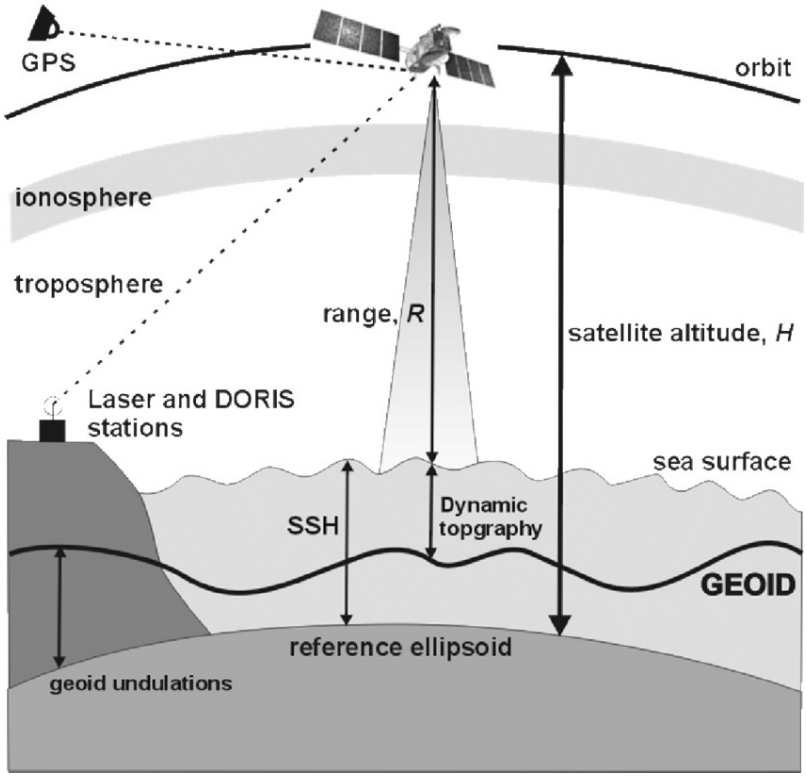

Figure 1: Principles of sea surface height measurements with satellite altimetry (from Volkov, 2004)

In order to get the SSH from the corrected range measurements obtained from the altimeter, a precise location of the satellite position is needed. The satellite orbit is defined relative to a fixed reference surface, the ellipsoid. A reference ellipsoid is a rough approximation of the earth's shape. Determining the precise location of the satellite is one of the most important factors that contribute to the error margin in altimetry data from satellites. Improvements in modelling earth's gravity field and satellite tracking systems have improved the range resolution in satellite altimetry greatly (Volkov, 2004). In oceanography, sea level is measured relative to the geoid. The geoid is an equipotential surface of earth's gravity field that represents the shape the ocean surface would have under the influence of gravity alone, in the absence of external forces such as winds, currents, or tides. In summary, to determine the sea surface elevation using satellite altimetry, three heights need to be known, the corrected range, the height of the satellite above the reference ellipsoid, and the

height of the geoid above the reference ellipsoid (Pugh, 1987). The different heights involved in satellite altimetry can be seen in Figure 1.

Swath altimetry has the possibility to improve the resolution of traditional altimeter satellites (Fu et al., 2006). Whereas the traditional altimeter maps the ocean in 1D, so only at the nadir, swath altimetry does the measurements over a broad swath. Consequently, because of the wide swath larger crossover coverage, the revisit time is shorter, which enhances the temporal resolution. Swat altimetry is needed to assess sub-mesoscale processes, such as ocean eddies, and to get satellite measurements of higher quality in coastal regions (Fu & Rodriguez, 2004). Radar interferometry is one method by which swath altimetry can be achieved (Rodriguez & Martin, 1992). This method uses the difference in signal path lengths between two radar antennas mounted on the satellite and separated by a known baseline (Figure 2). When a radar pulse reflects off a surface target, the returned signals are received by both antennas. The phase difference between the two received signals provides information about the angle of incidence of the reflection. Together with the measured range the horizonal position of the radar signal within the swath can be determined. The relative phase shift Φ between the two signals is related to the range difference Δr by Equation 1, with λ as the radar wavelength.

$$(1)\ \Phi = \frac{2\pi\Delta r}{\lambda}$$

The incidence angle θ is related to the range difference by Equation 2.

$$(2)\ \Phi = \frac{2\pi B \sin(\theta)}{\lambda}$$

The height h above a reference plain (e.g. an ellipsoid) can then be obtained with Equation 3, with H being the altitude of the satellite.

$$(3)\ h = H - r_1 \cos(\theta)$$

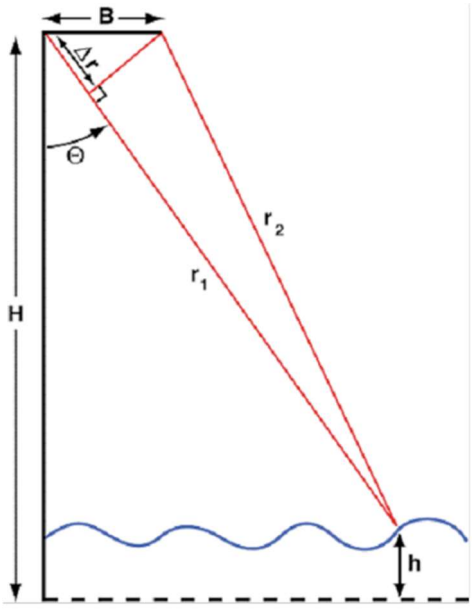

Figure 2: Geometric concept used for interferometric measurements (from Fu et al., 2012)

Interferometric measurements are subdue to random and systematic measurement errors. Random errors refer to non-systematic, unpredictable variations in measurements caused by instrument noise or environmental fluctuations. In radar interferometry, such stochastic errors affect the phase difference signal and can lead to small uncertainties in the derived surface elevation. The effect of random errors can be mitigated through spatial averaging. By averaging the measurements over a

number of adjacent pixels, the error is reduced in proportion to the square root of the number of pixels averaged. Besides, there are systematic measurement errors, which can be determined per pixel. There are three different kinds of systematic measurement errors that impact the interferometric measurements: range errors, roll errors, and systematic phase errors. Range errors are caused by similar processes that caused errors with radar altimetry measurements described earlier, so due to atmospheric refraction and the effects of the sea state. However, it should be noted that if you use the corrections determined from the nadir altimeter, the corrections vary across the swath. Roll errors arise from uncertainties in the roll angle of the interferometric baseline, causing a tilt in the measured surface across the swath. Measurement systems, such as an internal gyroscope, are capable of measuring the roll. Finally, phase errors are the result of variations in delays within the electronic system. The effect of these errors is similar to that of roll errors, causing linear tilt across the swath. Since these delay changes are mainly driven by slow temperature variations over an orbit, the systematic phase errors can be calibrated, similar to the roll errors (Fu & Rodriguez, 2004). The first time radar interferometry is used to make global observations of the water levels is the Surface Water and Ocean Topography (SWOT) mission.

1.3 Surface Water and Ocean Topography (SWOT) mission

The SWOT mission is a collaborative global survey of earth's surface water, conducted by the National Aeronautics and Space Administration (NASA) and the Centre National D'Etudes Spatiales (CNES) (NASA, n.d.). Since the launch of the satellite in December 2022 it has been collecting data of the water levels using radar interferometry technology. The missions two main objectives will contribute to both oceanography and terrestrial hydrology. High resolution, wide-swath altimetric measurements of ocean surface topography enhance the understanding of mesoscale and submesoscale oceanic processes. In tidal research, it is essential to accurately isolate the tidal signal from other sources of sea surface variability. Submesoscale processes can introduce small-scale noise that interferes with tidal signal extraction. Improved observation of these processes enables more effective filtering of non-tidal signals, leading to more accurate tidal reconstructions, especially in complex tidal environments. Additionally, measuring the terrestrial water elevation will give a better understanding of the spatial and temporal distribution of the storage and discharge of water on land (Fu et al., 2012).

There are two main data collection phases for the SWOT mission. The "fast-sampling" phase, or also known as the Cal/Val (Calibration and Validation) phase (January to July 2023), has a 1-day repeat orbit and has only visited certain areas of the world. This phase main purpose is the calibration and validation of the satellite. Additionally, the collected data can be used to study phenomena on a short temporal scale. The next phase started on July 21, 2023, for which the satellite had been brought in a different orbit. During this science phase, SWOT has a 21-day repeat period and a global coverage (SWOT Project, 2024). Due to the wide-swath and overlap in different tracks, on average the revisit time is around 11 days, depending on the location on Earth. The science phase provides a coverage of earth's surface waters up to 77.6° latitude over a swath of 120 km, with a nadir gap of 20 km. The resolution of the data is 2 km, although the unsmoothed data is also available at a 250 m native grid (JPL, 2025). This high-resolution data provides the opportunity to study several phenomena that where not yet possible with earlier datasets. SWOT can thus provide information to enhance the quality of tidal mapping in for example polar regions due to its larger inclination than TOPEX/Poseidon and Jason series (Table 1). Additionally, the high resolution of SWOT will improve the ability to measure sea level in presence of sea ice. The resolution of SWOT is also useful in near-coast and shelf environments. Because tidal wavelengths in shallow water are generally much shorter than those in the deep ocean, previous satellites with a lower resolution could not monitor them

accurately. Table 1 gives an overview of these different qualifications of SWOT compared to earlier satellite altimetry missions. The scientific data from the SWOT satellite is retrieved using several instruments, Table 2 gives an overview and a short description of the different applications (JPL, 2025).

Scientific instrument	**Function**
Ka-band Radar Interferometer (KaRIn)	Interferometer: range measurements across two 50 km swaths on each side of the nadir ground track.
Dual-frequency pulse-limited Nadir Altimeter (NAlt)	Nadir altimeter: range measurements along the nadir ground track.
three-frequency Advanced Microwave Radiometer (AMR)	Measures wet troposphere-induced range delays and atmospheric attenuation at Ku-, C-, and Ka-band frequencies. Range delays due to the dry troposphere are determined from meteorological models.
Doppler Orbitography and Radiopositioning Integrated by Satellite (DORIS) receiver	Determines satellite orbit. Measures the Doppler shift of radio signals emitted from a global network of ground-based beacons (NASA Earthdata, n.d.).
Global Positioning System Payload (GPSP) receiver	Tracking system: uses the GPS constellation of satellites to determine the exact position (CNES, n.d. a).
Laser Retroreflector Array (LRA)	Used to calibrate DORIS and GPSP: a passive instrument that acts as a reference target for laser tracking measurements performed by ground stations (CNES, n.d. b).

Table 2: Function of the scientific instruments on the SWOT satellite

1.4 Research based on SWOT data

Because the SWOT satellite mission is relatively new, the full range of its capabilities is not yet fully explored. However, there has already been some research published using the SWOT datasets that are related to the topics discussed in this paper. First, the accuracy of SSH measurements in coastal regions will be addressed. Second, an approach to reconstruct tidal characteristics using SWOT data is discussed.

The application of traditional satellite altimetry has always been challenging near the coast due to signal degradation and errors in corrections. Advancements in radar techniques and atmospheric and tidal corrections have enhanced the data quality in the coastal zone (Vignudelli et al., 2019). Still, the number of valid measurements increases with distance from the coast. Additionally, the quality of the data near the coast can be influenced by the angle between the satellite track and the coastline (Vignudelli et al., 2019). For example, Sentinel-3A data show higher percentage of valid sea level measurements when the ground track crosses the coast perpendicularly, reducing land contamination in the radar footprint (Figure 3 Vignudelli, 2019).

Due to SWOT's higher spatial resolution, improved performance in coastal regions is expected. Kupavõh et al. (2025) evaluated SWOT SSH measurements in the coastal areas of the Baltic Sea by comparing the 'Basic' data products with geoid-referenced tide gauge records. The study reported relatively low RMSD, averaging around 13cm. The RMSE did not significantly differ depending on the distance from the coast. However, in the near-coast area (0-2km), only about 40% of the datapoints where qualified as valid datapoints, in contrast to the 97% of the total dataset. It is mentioned that the low number of valid data points could be caused by the grid size limitations (2x2km) and relatively strict filtering. Using the 'Unsmoothed' version of the data (grid of 250 x 250m), better results could be achieved. However, SWOT still showed better results than previous satellite altimetry missions, such as Jason-3 and Sentinel-3A, who showed the same number of valid points within 7-

10km and 2-3km from the coast respectively (Kupavõh et al., 2025). This highlights that, despite advancements, land contamination remains a significant challenge for SWOT in coastal applications.

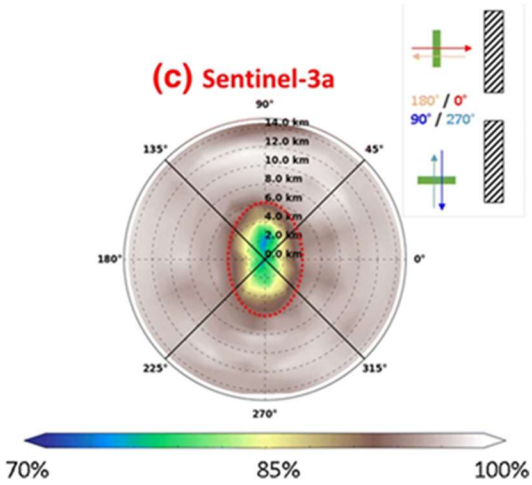

Figure 3: Percentage of valid measurements for Sentinel-3A datasets. The radius of the circle corresponds to the distance of the measurement from the closest coastline. The perimeter of the circle corresponds to the angle formed between the ground track of the satellite and the closest coastline (from Vignudelli et al., 2019)

Satellite altimetry has historically faced challenges in coastal tidal analysis due to limited temporal and spatial resolution and reduced accuracy near the coast. Hart-Davis et al. (2024) used SWOT Cal/Val data with a near daily repeat to perform a tidal analysis in two coastal regions: the Bristol Channel and Great South Bay. Their results showed notable improvements over existing tide models, with typical errors in the range of tens of centimetres and degrees. When validated against in situ tide gauges, SWOT-derived M_2 tidal estimates showed amplitude errors of just 1.75-3cm and phase differences of 1.75°-2.75°.

The analysis made use of aliased tidal signals. With a repeat cycle of 0.9935 days, the dominant M_2 tide (period of 12.42 hours) was aliased to a period of approximately 12.4 days. This provided eight full cycles of the aliased M_2 tide within the observation window of 102 days. Several constituents have an alias period close to that of the M_2 constituent, which could impact the estimation. But since these constituents are indicated to have an amplitude which is only a fraction of the M_2 tide, its impact is expected to be minimal. Although there were only 87 satellite observations available, they still managed to perform a harmonic analysis in both regions (Hart-Davis et al., 2024).

In this thesis, the performance of the SWOT satellite in the Dutch North Sea (shelf sea) and Wadden Sea (intertidal area) will be examined using the oceanography product. Previous satellites that used radar altimetry have shown to have difficulties in coastal areas (Vignudelli et al., 2019). The first aim will thus be to validate the SWOT satellite measurements using in-situ tidal gauge measurements from Rijkswaterstaat (RWS), the Dutch water authority.
The second aim of this paper is to determine to what extent the SWOT data is useful to determine tidal dynamics in coastal areas and on a large spatial scale. A different approach for reconstructing the tidal signal using SWOT data is introduced. Based on a representative tidal cycle, the tidal signal in the North Sea will be retrieved.

The following research questions will be answered:

1. How accurate is SWOT in measuring sea surface height in the Dutch coastal environment?
2. What is the potential of SWOT satellite data for retrieving the tidal signal in the North Sea?

The first part of this paper discusses the datasets used and outlines the method for validating the SWOT data and reconstructing the tidal signal. The second part first discusses the results of the validation, which are compared with known accuracies from previous satellite altimetry missions and other studies using SWOT data. Then the result of the tidal reconstruction is presented and the method used in this paper is compared with other possible methods that use SWOT data as well.

2 Methodology

2.1 Datasets

For this research several datasets are used for data extraction and validation. The most important are the dataset of SWOT satellite measurements and the tidal gauge data from RWS. Additionally, datasets are used to determine the height differences between different ellipsoid and geoid levels. This section will elaborate more on the specifics of these different datasets and why these datasets are used for the research.

SWOT satellite data

The SWOT mission provides two main types of SSH data products derived from the KaRIn: the High Rate (HR) and Low Rate (LR) datasets (JPL, 2025). Both products are based on swath measurements from KaRIn, which captures two-dimensional SSH observations across a wide swath of 120 km, excluding a 20 km nadir gap. The HR datasets offer measurements on KaRIn's native grid, with a spatial resolution of approximately 250 to 500 metres depending on the distance from the nadir. The resolution differs with distance from the nadir because of the range errors explained in section 1.2. These datasets retain fine-scale variability and are particularly suited for observing inland water bodies, small-scale oceanographic processes, and complex coastal environments. In contrast, the LR datasets provide SSH observations that have been filtered, smoothed, and resampled onto a 2km x 2km grid. Although coarser, the LR product is optimised for open-ocean and coastal applications, including sea level studies and tidal signal analysis. The data obtained from the onboard altimeter is available in a different data product but will not be used in this study. For this research, the following dataset is used: SWOT_L2_LR_SSH_EXPERT_2.0 (Surface Water Ocean Topography (SWOT), 2024). This dataset provides low rate (LR) global SSH and significant wave height observations from the KaRIn. The L2 SSH data product is given in one netCDF-4 file per pass. A pass is a half-orbit, covering the full swath width. Different parameters are given, such as the sea surface height, sea surface height anomaly relative to the mean sea surface, wind speed and significant wave height. The parameters are given on a geographically fixed, swath-aligned 2km x 2km grid (CNES, n.d. c). This research makes use of the Expert dataset because it provides multiple parameters that can be used for quality checking, but it needs minimal smoothening. Several variables from the SWOT dataset have been used in this research. Table 3 provides an overview of these variables along with their definitions (SWOT, 2023). The spatial grid is structured by a series of 'lines' along the satellite's flight path (along track) and 'pixels' across the swath (across-track). Consequently, each variable is represented as a two-dimensional array corresponding to this spatial grid of measurements (NASA PODAAC, 2023). The SSH measurements given by the ssh_karin_2 variable need to have an additional height correction from crossover calibration. Also, the geoid height needs to be subtracted, to get the SSH relative to the geoid. This is done according to Equation 4.

$$(4)\ SSH_{SWOT} = SSH_{karin\_2} + xover\ corr - h_{geoid}$$

Variable	Definition
ssh_karin_2	SSH measured by KaRIn, with corrections applied, and is given relative to the reference ellipsoid, World Geodetic System 1984 (WGS 84).
height_cor_xover	Height correction from crossover calibration. In order to correct systematic errors or biases in the height measurements.
geoid	Geoid height above the reference ellipsoid, including the permanent tide.
ssh_karin_2_qual	Gives the quality flag for the SSH.
height_cor_xover_qual	Gives the quality flag for the crossover calibration.
latitude	Degree's north (positive) or south (negative).
longitude	Degree's east (0°-360°).
Time	Time of measurement in seconds (UTC time scale) since 1 January 2000

Table 3: Different variables that are used from the SWOT_L2_LR_SSH_EXPERT_2.0 dataset.

Rijkswaterstaat tidal gauge data

For the validation of the SWOT measurements, in-situ SSH data from tidal gauges operated by RWS are used. The data from the various stations is publicly available via waterinfo.rws.nl. Figure 4 shows the locations of the tidal gauge stations that were used for this research. The stations are divided in three groups, each have their own challenges and expected accuracy results. Appendix A shows the coordinates per tidal gauge station The North Sea stations are located further from the coast, hence expected to have the best results. However, since the North Sea is a shelf sea, it is still a challenging environment (e.g. Volkov et al., 2007). The coastal stations are expected to have the largest errors stemming from land dispersion (e.g. Kupavõh, 2025). The stations located in the Wadden Sea are also expected to have larger errors, since this is a large intertidal area and also close to the coastline. Because of the effect of land dispersion, for the stations located at the coastline, a coordinate for the SWOT measurements is chosen completely in the sea, but still close to the tidal gauge location. The exact choice of the location might impact the result of the validation and should thus be handled with caution. At each station, water levels are recorded at 10-minute intervals. However, not all stations provide continuous time series data over the full research period. Each measurement has been checked for quality; measurements flagged with a measurement error were excluded from the analysis. Water levels are referenced either to the Normaal Amsterdams Peil (NAP) or to Mean Sea Level (MSL). However, MSL is not uniformly defined across all stations (Rijkswaterstaat, 2010). NAP is the Dutch vertical datum and is approximately equal to the geoid height. The geoid model for these measurements has an accuracy of better than 3 cm (Hydrographic Service Ministry of Defence, 2020). During this research, the water levels referenced to NAP will be used. These can be easily transferred to other reference levels.

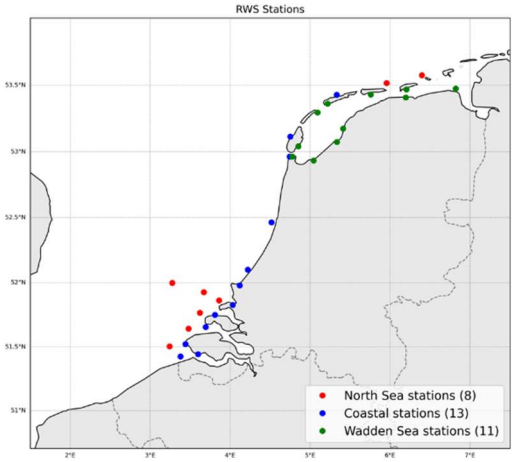

Figure 4: Used tidal gauge stations from Rijkswaterstaat.

Other datasets

To transform the water level data from RWS to the same vertical reference frame used in SWOT, additional datasets were used. The NLLAT2018 grid from the Hydrographic Service of the Ministry of Defence was used to reference NAP to the WGS84 ellipsoid. The transformation between the ellipsoid and the EGM2008 geoid was obtained using the GeographicLib online geoid evaluator (https://geographiclib.sourceforge.io/C++/doc/GeoidEval.1.html). For both transformations, the coordinates of the tidal gauge stations from RWS were used. Additionally, to spatially constrain the analysis to the North Sea, a shapefile was used based on the Marine Regions Geographic Identifier (MRGID:2350), corresponding to the North Sea area as defined by the International Hydrographic Organization (IHO). This dataset can be found here: http://marineregions.org/mrgid/2350. Equation 5 gives the transformation of RWS SSH measurements to the same reference level as SWOT satellite measurements.

$$(5)\ SSH_{RWS} = SSH\ (NAP) + conversion\ NAP\ to\ ellipsoid\ (WGS84) - conversion\ to\ geoid\ (egm2008)$$

The results of this conversion have been used for the rest of the analysis in this study.

2.2 Data validation

In this section the method for validation of the SWOT data using tidal gauge measurements from RWS is discussed. For each SWOT pass, the closest measurement in time from RWS is taken. Then within the SWOT dataset, the closest coordinate to the tidal gauge station is selected. Missing values in the RWS or SWOT dataset are removed in both the datasets. In the SWOT data, some values of ssh karin 2 and the crossover correction are flagged as not good quality. These values are also flagged in the analysis. The number of 'good quality' datapoints gives an indication of the overall quality of the measurements. To assess the performance of SWOT-derived SSH, three statistical metrics were calculated: the coefficient of determination (R^2), the mean bias, and the root mean square error (RMSE). R^2 quantifies how well SWOT captures the temporal variability of sea level observed at RWS stations (Equation 7), while the bias identifies systematic height offsets (Equation 8). RMSE provides a combined measure of accuracy, incorporating both random and systematic discrepancies (Equation 9). For the bias and the RMSE, a relative value is also given, in which the bias or RMSE are calculated as percentage of the local tidal range. In this analysis, the slope of the regression line was fixed at 1, only the intercept was estimated from the data. The slope can be fixed at 1, based on the assumption that both SWOT and RWS measurements capture the same temporal variations in sea level. This means that any differences between the two datasets are not due to differing trends over time but are instead attributed to measurement offsets or noise within the systems. By fixing the slope, the comparison is limited to the offset (intercept) and the residual variation between the two measurement methods. Given the SWOT values x_i and the RWS values y_i, the fitted line is computed as:

$$(6)\ \hat{x}_i = m \cdot y_i + intercept$$

with m equal to 1.

From this, the statistical indicators are computed, with *n* the number of datapoints:

$$(7)\ R^2 = 1 - \frac{\sum_{i=1}^{n}(x_i - \hat{x}_i)^2}{\sum_{i=1}^{n}(x_i - \bar{x})^2}$$

$$(8)\ bias = \frac{1}{n}\sum_{i=1}^{n}(y_i - x_i)$$

$$(9)\ RMSE = \sqrt{\frac{1}{n}\sum_{i=1}^{n}(y_i - x_i)^2}$$

The statistical indicators are computed for each tidal gauge station of RWS in the Dutch seas and at the coasts. Additionally, a scatter plot is made for a visualisation of the spread of the measurements.

2.3 Harmonic analysis

This study used approximately 1.5 years of SWOT satellite data, with one measurement per location every 11 days on average. Due to the sparse temporal resolution, harmonic analysis is not readily applicable. Therefore, a representative tidal cycle is constructed, enabling the application of harmonic analysis despite the limited sampling frequency of SWOT.

To construct a representative time series, all SWOT measurements are referenced to the timing of the previous local high water. For this, the continuous RWS time series at Vlakte van de Raan is used as a reference, as it provides SSH measurements at 10-minute intervals. High water events are extracted from this dataset and used as temporal reference points. This is done using the find_peaks function from SciPy library (https://docs.scipy.org/doc/scipy/reference/generated/scipy.signal.find_peaks.html). Each SWOT measurement is expressed as the time difference relative to the nearest prior high-water event at Vlakte van de Raan. This approach creates an effective representation of all measurements into one tidal cycle. However, it assumes that the North Sea exhibits predominantly semidiurnal tidal behaviour, which is also expected for the region (Pugh, 1996).

Longer period modulations, such as the spring-neap cycle, are not captured in this analysis. These arise from the interference of multiple constituents (e.g. M_2 and S_2). To prevent distortions of this effect in the fitted tidal signal, a normalisation step has been applied prior to harmonic fitting. To apply the normalisation for the spring-neap tide effects on the SSH measurements of SWOT, the local tidal range and average spring tidal range are used. The correction factor is defined in Equation 10.

$$Corr\ factor = \frac{HW_{local} - LW_{local}}{Avg\ spring\ range} \quad (10)$$

This correction factor is determined for each dataset, which has approximately the same observation time for each measurement. Then on each SSH measurement, the correction factor is applied to (Equation 11).

$$ssh\ scaled = ssh \cdot \frac{1}{correction\ factor} \quad (11)$$

This now gives a reconstructed representative tidal signal, in which each SSH measurement is scaled for spring-neap tidal effects. The UTide package (Codiga, 2011), version 0.3.0 was used to perform harmonic analysis of the tidal signal. This toolbox enables least-squares fitting of tidal constituents to unevenly sampled time series, making it suitable for this project. The ut_solve() function was used to estimate the tidal parameters (amplitude and phase for M_2 and M_4 tidal constituents. It fits the sinusoidal model directly to the time series using a least-squares method.

Using the approach described above, the tidal characteristics are determined at the location of multiple tidal gauge stations. This is done using the SWOT data and the RWS data in order to compare the results and determine the applicability of this method. Furthermore, the same method has been applied to SWOT data over the North Sea. Here, high water moments at Vlakte van de Raan are taken as reference. To increase the effective number of observations, the study area is divided into grid cells of 5x5km. This spatial resolution still allows for effective representation of tidal dynamics. Each grid cell contains measurements of multiple SWOT passes over a 1.5-year period. With the resulting amplitude and phase, a map is created visualising the distribution of the tidal parameters over the North Sea.

With use of the results of the harmonic analysis of the North Sea, a SSH map is reconstructed based on the dominant M_2 tide. The reconstruction assumes a purely harmonic tidal signal, described as a cosine function of time. For each grid cell, the instantaneous SSH at a given time t (in hours) was calculated using Equation 12.

$$SSH(t) = A \cdot \cos(\omega t - \varphi) \quad (12)$$

where:

- A is the M_2 amplitude
- $\varphi$is the M_2 phase (converted to radians)
- $\omega$is the angular frequency of the M_2 constituent ($\omega = \frac{2\pi}{T}$, with T = 12.42 hours)
- t is the time since local high water at Vlakte van de Raan

3. Results

This section presents the results of the data validation of the SWOT satellite measurements and the harmonic analysis of the SWOT SSH data in the North Sea. First, the accuracy of the radar interferometry-derived satellite data is assessed by comparison with in-situ tidal gauge measurements from RWS. For several measurement stations, scatter plots of the SWOT versus RWS water levels are shown, accompanied by statistical indicators. Next, the results of the harmonic analysis of the M_2 and M_4 tidal component in the North Sea are visualised. Finally, the reconstructed SSH for the North Sea based on the tidal reconstruction is presented.

3.1 Data validation

The comparison between SWOT observations and in-situ RWS measurements reveals notable differences across three different environments: the open North Sea, the coastal North Sea, and the Wadden Sea. This section first summarises the overall quality of SWOT data, followed by representative scatter plots for each environment to illustrate measurement variability. Appendix B presents the scatter plots for each tidal gauge station.

Table 4 presents the validation statistics per group and for the combined dataset. The coefficient of determination (R^2), reflecting the correlation between SWOT and RWS SSH values, is strong across all groups, with an average R^2 of 0.88. The average RMSE is 0.22 m, equivalent to approximately 10% of the local tidal range. However, there are significant regional variations. The Wadden Sea exhibits a lower R^2 value of 0.79, compared to 0.98 in the open sea and 0.92 at coastal stations in the North Sea, indicating reduced data quality in this intertidal environment.

The bias, representing the mean offset between SWOT and RWS SSH values, is consistently negative across all stations, suggesting a systematic overestimation of SSH by SWOT. The bias is smallest in the open North Sea (-0.08m), followed by coastal stations (-0.10m). However, variability between different measurements is higher, likely due to differing choice of measurement locations aimed at mitigating land contamination. In the Wadden Sea, the bias is greatest (-0.22m). Expressed relative to the local tidal range, the bias remains relatively low across all regions, with an average of 7.8% of the local tidal range.

The RMSE, a combined measure of accuracy, is also regionally dependent. It remains relatively low in the open sea (0.14m) and at coastal stations in the North Sea (0.16m) but is notably higher in the Wadden Sea (0.34m). Relative RMSE values are also provided for comparison across different tidal regimes. Finally, the percentage of SWOT observations classified as high quality diminishes from 48%

in the open sea to 6.3% at coastal stations, and just 0.8% in the Wadden Sea. This trend clearly shows that the proportion of good quality SWOT data decreases progressively from offshore regions towards the coast and into more complex, intertidal environments. Importantly, data not flagged as high quality may still be usable but requires careful interpretation due to potential complications.

Stations	*North Sea*	*Coastal*	*Wadden Sea*	*Total*
R^2	0.98	0.92	0.79	0.88
Bias	-0.08m (-3.2%)	-0.10m (-6.0%)	-0.22m (-12.1%)	-0.14m (-7.75%)
RMSE	0.14m (5.0%)	0.16m (8.8%)	0.34m (14.1%)	0.22m (10.0%)
% good quality	48%	6.3%	0.79%	13.7%

Table 4: Summary of validation of SWOT and in-situ (RWS tidal gauge) derived SSH measurements.

As indicated before, the stations located in the open North Sea show a strong agreement between the different tidal gauge stations. Vlakte van de Raan is representative of this group and is also used in further tidal analysis. In the associated scatter plot (Figure 5) the SSH value for both the SWOT data and RWS data are indicated, along with a 1:1 reference line (red) indicating a perfect fit. The green line indicates the best fit for the harmonic analysis.

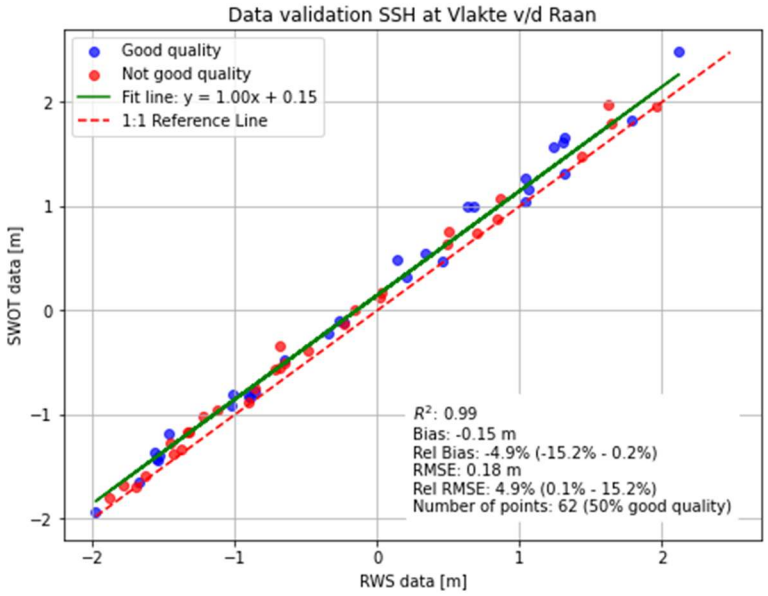

Figure 5: Scatter plot of Vlakte van de Raan. Indication of SSH measured by SWOT and RWS, and if SWOT has qualified the measurement as 'good quality' (in blue).

For the coastal group, the bias and RMSE are similar to the North Sea stations. However, the amount of good quality SWOT datapoints is substantially lower. Moreover, the choice of exact coordinate for the SWOT measurement has a pronounced impact on the result. This problem is important for this group, since the normal, exact coordinates of the station cannot be used due to land contamination. Therefore, another coordinate slightly off the coast needs to be chosen. Figure 6 shows the difference between two different choices for the exact location for the same tidal gauge station. Figure A is closer to the coastline, while Figure B is slightly more offshore. Location A yields lower correlation

and a higher RMSE, while location B shows a lower bias and improved correlation. A lower bias suggests reduced overestimation of SSH by SWOT. These differences highlight the importance of site selection when assessing SWOT performance in coastal zones.

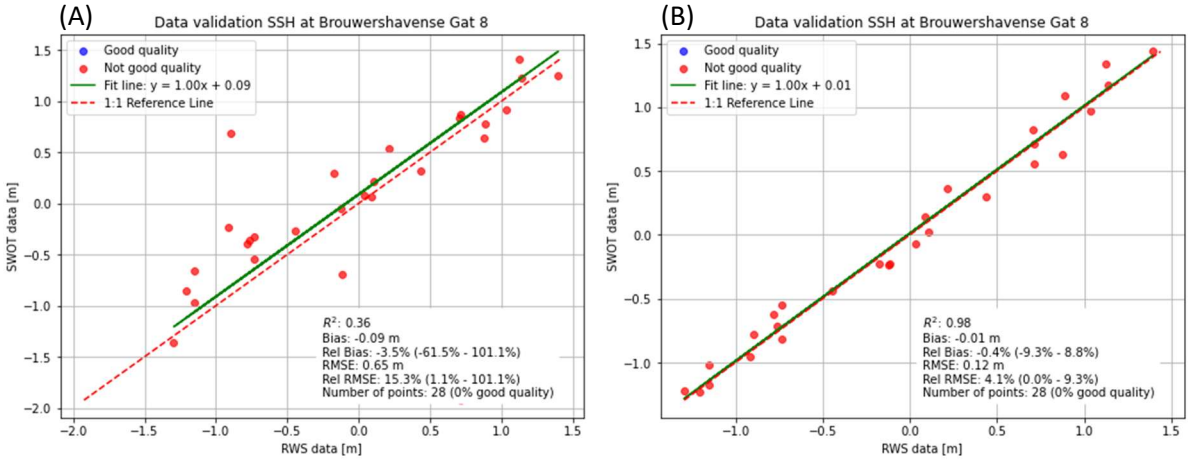

Figure 6: Scatter plot of Brouwershavense Gat 8. A) indicates the validation for a coordinate close to the coast. B) indicates the validation for a coordinate further from the coast.

In the Wadden Sea, the overall agreement between SWOT and RWS data is considerably poorer. The scatter plot for Schiermonnikoog (Figure 7) supports this conclusion. Notably, a distinction emerges between high tide (SSH > 0m) and low tide (SSH < 0m) measurements. High tide observations exhibit less scatter, indicating improved quality during these periods.

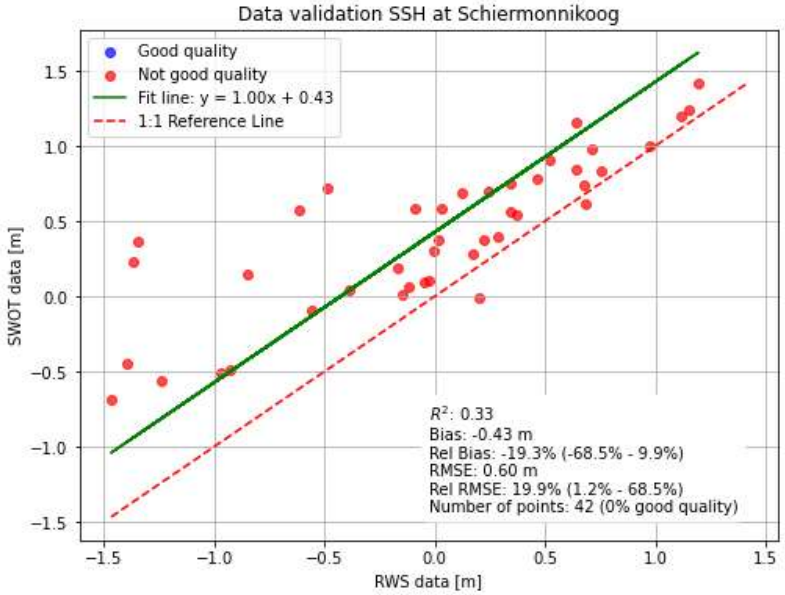

Figure 7: Scatter plot of Schiermonnikoog.

3.2 Harmonic analysis in the North Sea

First the harmonic analysis using a representative tidal cycle is done per tidal gauge station. The results can subsequently be compared with a harmonic analysis performed applying the same methodology, only using RWS in-situ measurements. For this part, the M_2 and M_4 tidal constituent are used in the analysis. The results for Vlakte van de Raan are displayed in Figure 8. The R^2 value is 0.96, indicating a good correlation of SWOT measurements and the reconstructed tidal signal. The bias between the reconstruction of the tidal signal using SWOT measurements and RWS measurements is 0.20m, with a RMSE of 0.21m. Thus, the reconstructed SSH of the tidal signal is higher using SWOT

data, with a RMSE in the same order of magnitude. When we include the bias found in the SSH measurements at Vlakte van de Raan (-0.15m), the resulting difference is minimal.

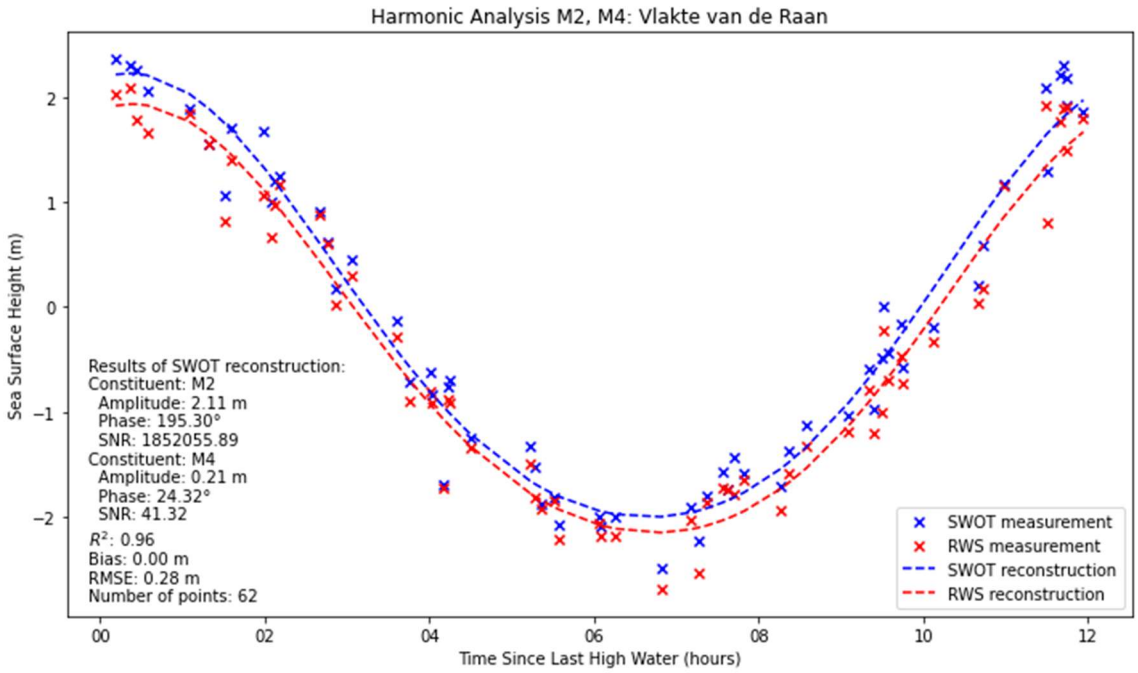

Figure 8: Result of harmonic analysis of the SWOT data (blue) and RWS data (red) at the location of Vlakte van de Raan. The dotted lines indicate the best fit of the M_2 and M_4 tide combined.

At the station of Europlatform, the effect of including both the M_2 and M_4 tidal constituents is clearly visible (Figure 9). Figure A shows the tidal reconstruction using only the principal lunar semi-diurnal constituent (M_2), which is the dominant constituent in the North Sea tidal regime. The M_4 tidal constituent, known as the shallow water overtide of M_2, has a period of half that of M_2 (6.21 hours). It arises from the non-linear distortion of the M_2 wave in shallow or coastal waters and contributes to the asymmetry of the tidal curve. When the M_4 constituent is included in the analysis, the result is a steep falling limb (ebb) and a slower rising limb (flood). The observed phase lag of 212° means that M_4 peaks shortly after M_2 reaches high water, leading to an ebb-dominant asymmetry in the tidal signal.

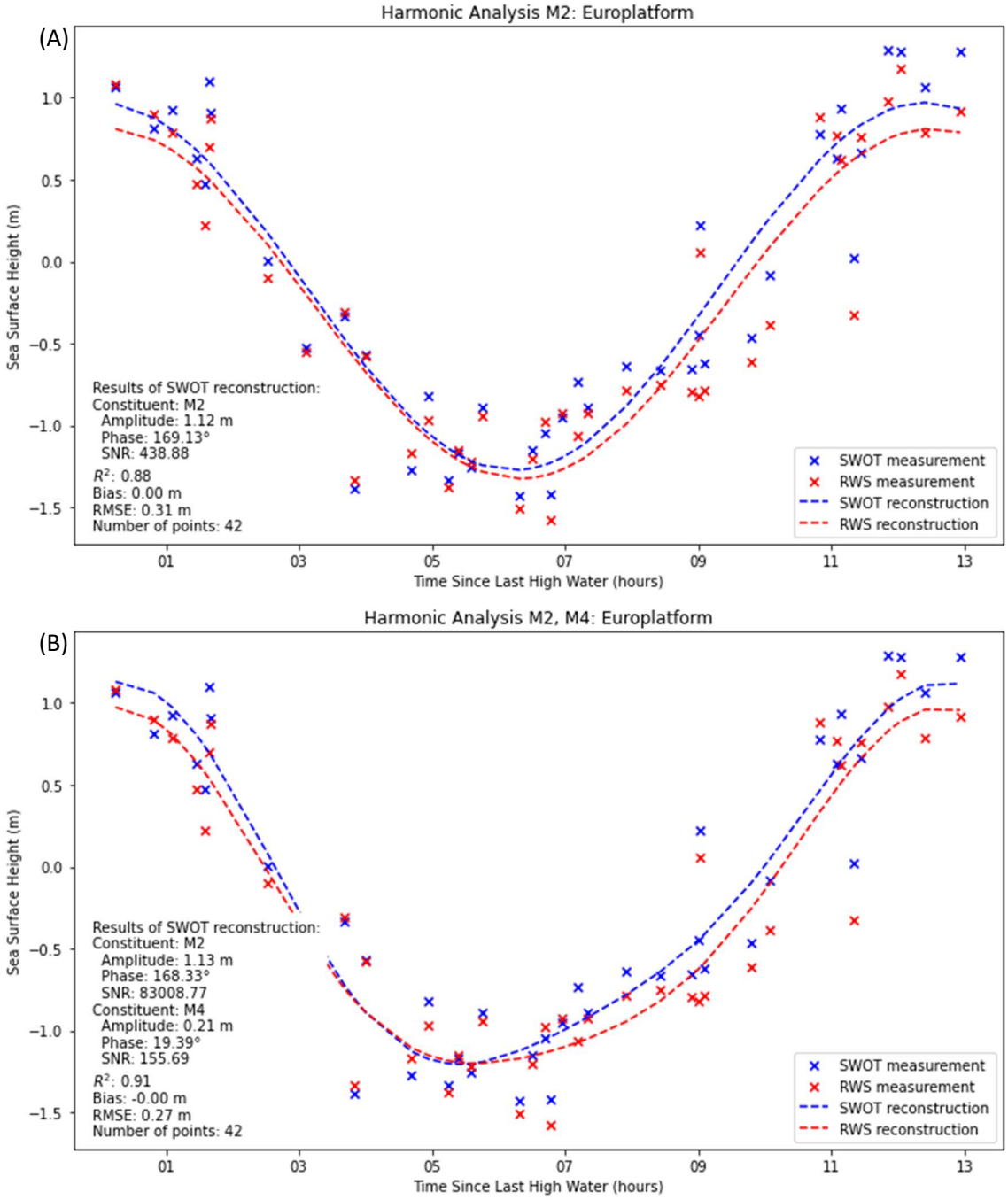

Figure 9: Result of harmonic analysis of the SWOT data (blue) and RWS data (red) at the location of Europlatform. The dotted lines indicate the best fit of the M_2 (Figure 9A) and M_4 (Figure 9B) tide.

When the harmonic analysis is extended over the North Sea, where for each grid cell a representative tidal cycle is created with Vlakte van de Raan as reference for high water times, it is possible to see the patterns of tidal amplitude and phase. Figure 10 shows the result of this tidal analysis for the M_2 tidal constituent using SWOT data. In this map, the colours represent the tidal amplitude in metres, the white lines indicate the phase in degrees. Several characteristics of tidal systems in the North Sea are recognizable. Two amphidromic systems are clearly identifiable, one in the central North Sea and another in the southern basin. These points, where tidal amplitude approaches zero, are characteristic of the semidiurnal tidal regime. They mark centres around which the M_2 tidal wave rotates. The cotidal lines radiating outward from these amphidromic points illustrate the progressive phase propagation of the tidal wave through the basin. Along the Dutch coast, the tidal wave

propagates from south to north, as expected. Amplitudes increase towards the coast, reflecting the influence of shoaling and resonance in shallow waters. Especially in the English Channel, the geometry acts as a bottleneck, amplifying the tidal amplitude in this region due to resonance and wave convergence.

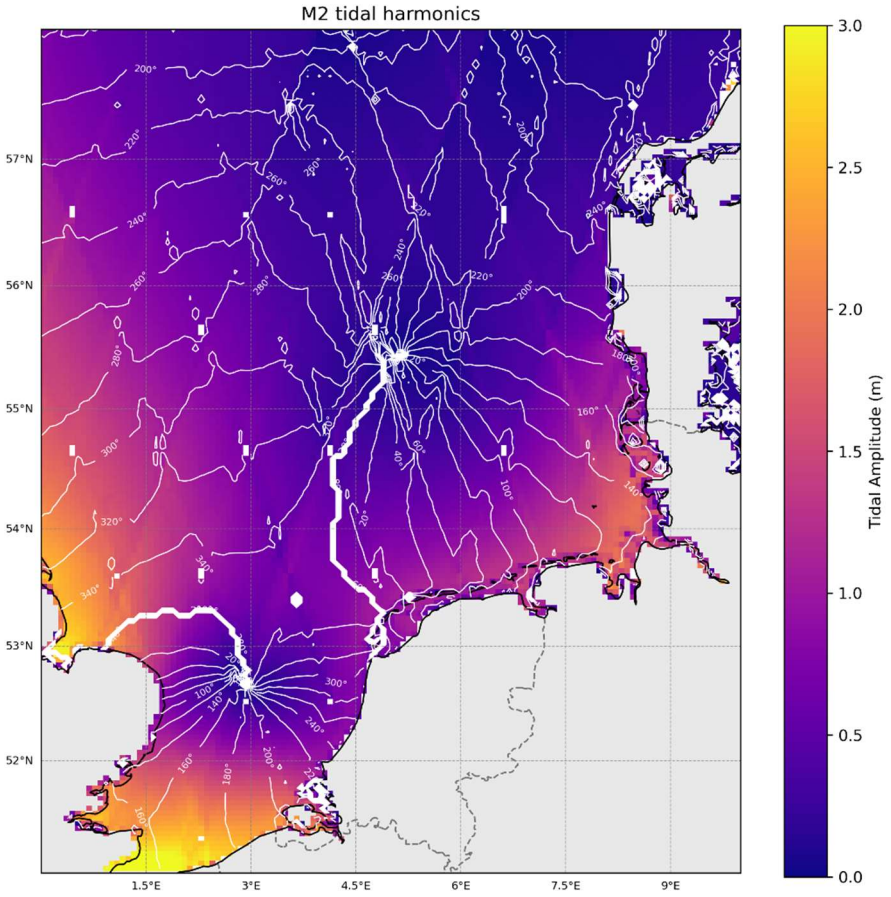

Figure 10: North Sea M_2 tidal characteristics obtained from SWOT measurements. The colour scale indicates the amplitude, and the white lines indicate the phase.

While the harmonic analysis captures the dominant spatial patterns, some inaccuracies are apparent. In coastal regions, especially in complex estuarine zones and intertidal regions, the amplitude field appears less smooth. This is likely due to limitations in spatial resolution and land contamination of the SWOT measurements. Additionally, in the map, the lines where the nadir of SWOT passes is located are visible. They are apparent because of sharp colour transitions or sudden jumps in cotidal phase lines. These discrepancies can be caused by under-sampling in these points, since there are no measurements in the nadir, it lacks data of one SWOT pass, significantly decreasing the amount of datapoints. Additionally, the use of fewer datapoints for the harmonic analysis increases the vulnerability for outliers and errors in the data.

The Signal-to-Noise Ratio (SNR) is a method to indicate the strength of the tidal signal compared to background noise, such as wind, waves or other disturbances. Figure 11 shows the SNR for the harmonic analysis using the M_2 tidal constituent. This clearly indicates the differences between different SWOT passes. Some passes have a significantly higher SNR then others, this might be due to the circumstances during the measurements, such as surges that influence the signal. Additionally, the amphidromic points can also be distinguished. They have a distinctively lower SNR then their surroundings, suggesting that these areas are harder to reconstruct using this methodology. Although

in general, the SNR has a good value, indicating that the harmonic analysis was successful. Most values for the SNR are well above 2, which is generally considered a good value.

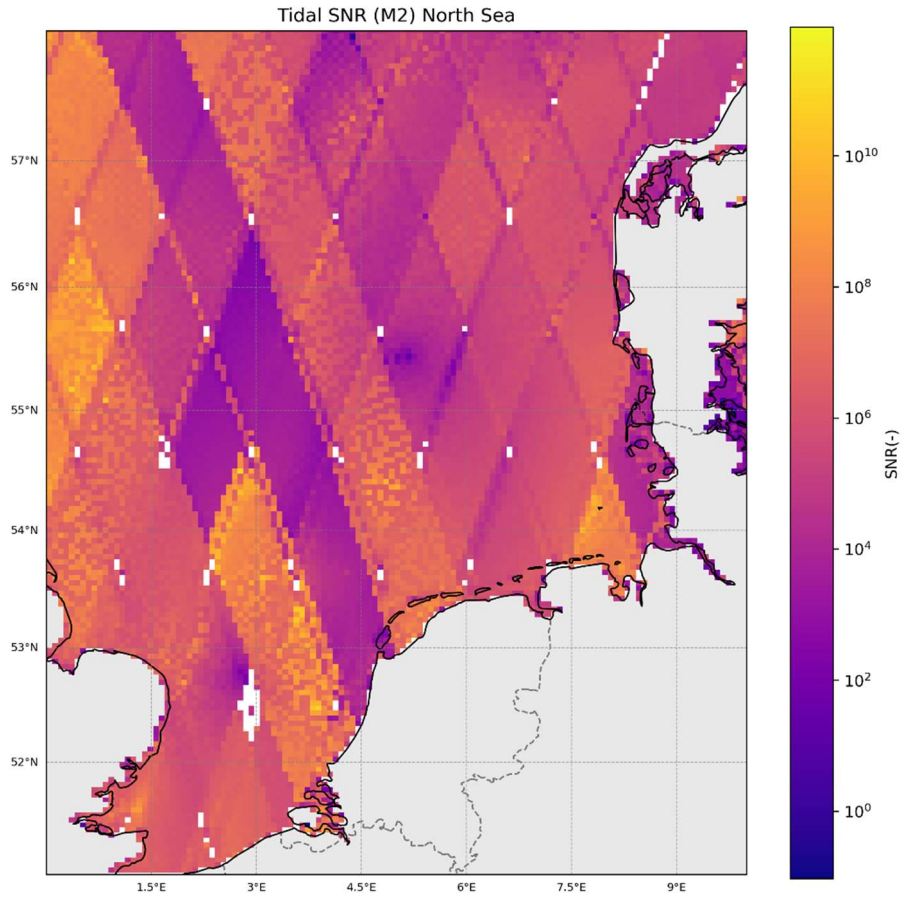

Figure 11: North Sea M_2 signal-to-noise ratio obtained from the harmonic analysis.

Figure 12 presents the spatial distribution of the M_4 tidal constituent amplitude across the North Sea. The M_4 constituent exhibits relatively low amplitudes compared to M_2, with peak values generally below 0.3 metres. Elevated M_4 amplitudes are primarily concentrated along coastal zones and shallow bathymetric features, particularly in the English Channel and the eastern boundaries of the basin. These patterns are consistent with areas where tidal distortion is enhanced by frictional effects and resonance in confined geometries. The regular, diamond-shaped interference pattern observed offshore, in regions with low M_4 amplitudes, suggests underperforming of the harmonic analysis in these areas. It indicates that in regions where nonlinearity is weaker and M_4 generation is minimal, the accuracy is reduced. The SNR for the M_4 tidal constituent (Figure 13) is also lower than that of the M_2 constituents, although it is generally still above 2. However, there are also some substantial areas with a SNR value indicating that the constituent fit is not very reliable (SNR<<2) for those locations.

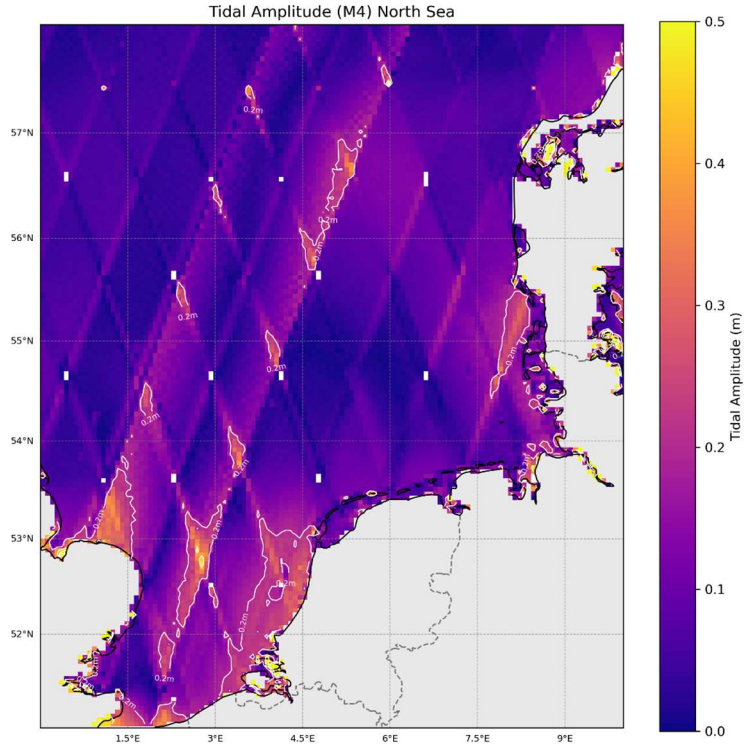

Figure 12: North Sea M_4 tidal characteristics obtained from SWOT measurements. The colour scale indicates the amplitude, and the white lines indicate isopleths of same amplitude.

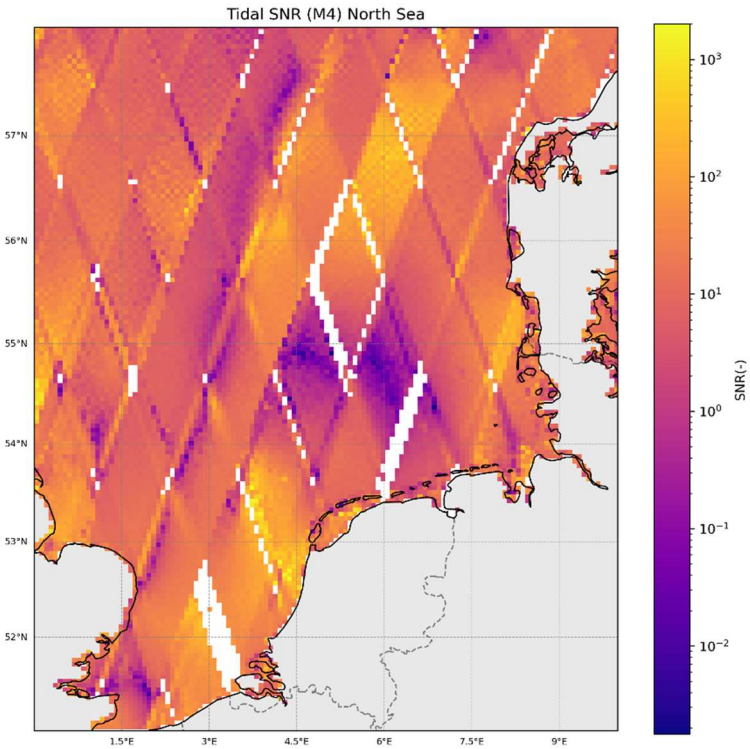

Figure 13: North Sea M_4 signal-to-noise ratio obtained from the harmonic analysis.

3.3 Sea surface height obtained from harmonic analysis

Using the results of the harmonic analysis, it is possible to reconstruct SSH in the North Sea at specific moments within the tidal cycle. Figure 14 presents SSH at 3-hour intervals, while Appendix C contains the full sequence of hourly reconstructions. These visualisations illustrate the propagation of the tidal waves throughout the North Sea. High water at Vlakte van de Raan is used as the temporal reference point for each reconstruction, similar to the tidal reconstruction with the harmonic analysis. The tidal wave can be observed propagating northwards along the Dutch coastline and southwards along the English coastline. The anticlockwise rotation around the amphidromic point is clearly identifiable, as is the formation of a Kelvin wave within the English Channel. Furthermore, the reconstruction reveals larger tidal ranges in coastal areas, with more pronounced high and low water levels near the coast.

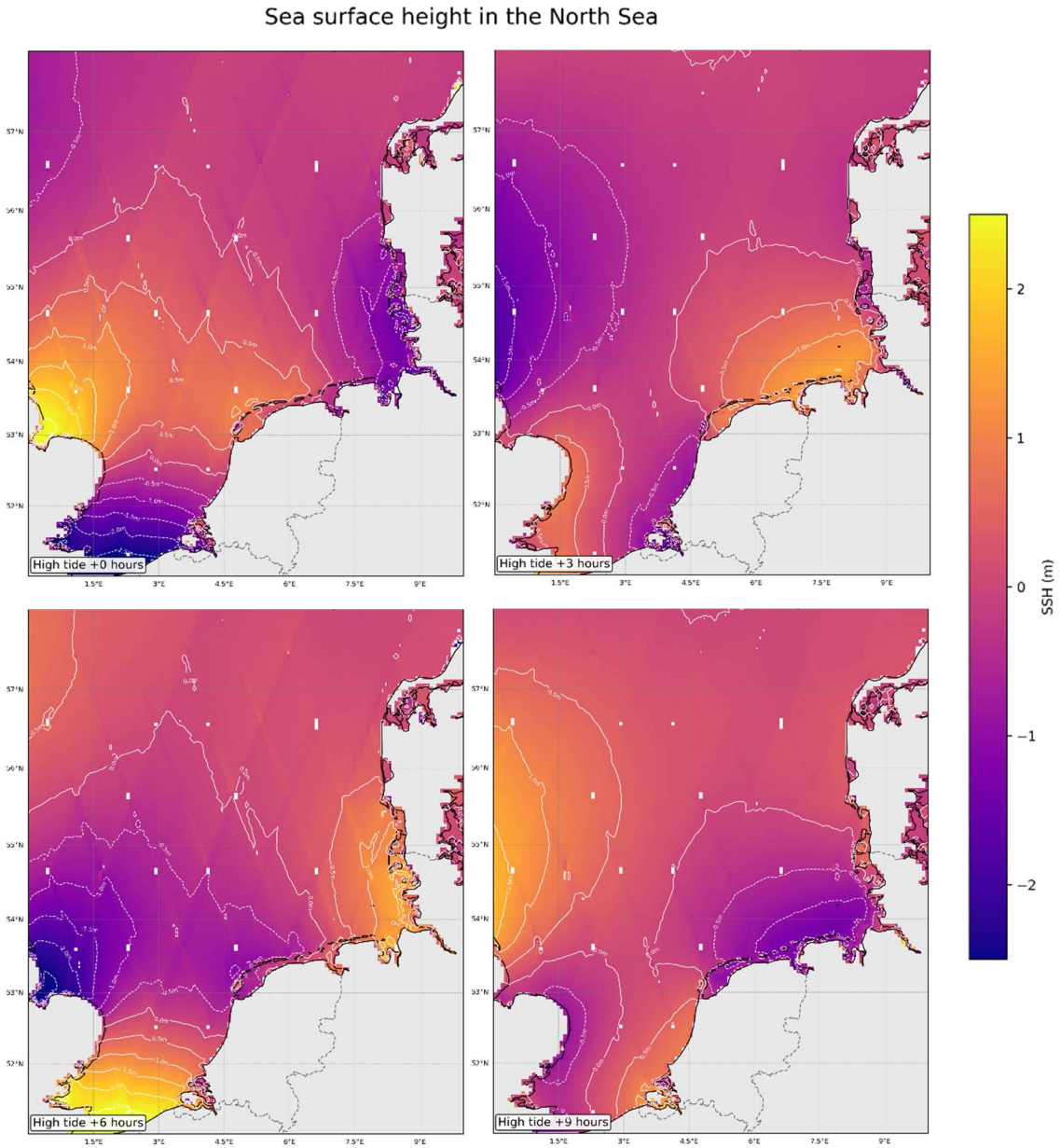

Figure 14: Sea surface height (SSH) derived from the M_2 tidal characteristics based on SWOT data. The SSH is given at time intervals of three hours, starting with high water at Vlakte van de Raan.

4. Discussion

In this chapter, the results will be discussed and put into perspective of broader research. First, the results of the data validation will be evaluated using other SWOT studies and previous satellite altimetry missions. Second, the results of the harmonic analysis will be put into perspective. The method used in this research, with a representative tidal cycle, will be compared to other methods.

4.1 Data validation

The expected vertical accuracy for SWOT in oceanographic applications is generally within a few centimetres (~5-10cm) over open ocean, under optimal conditions. Over coastal and enclosed seas, however, the accuracy tends to degrade due to increased topographic complexity, land contamination, and high-frequency variability not fully captured by SWOT. These results align with these expectations. Overall, the correlation between SWOT and RWS measurements is strong (R^2 = 0.88). The bias is determined to be -0.14cm on average, and this seems to be relatively consistent across the different stations. This indicates that the SWOT measurements consistently overestimate SSH, which suggests a measurement error or an error in the conversion of the reference level between the SWOT and RWS measurements. Since the Cal/Val phase has already been completed and during this time, the measurements have been calibrated, the most likely cause is an error in the conversion of heights.

The RMSE is found to be 0.22m, with the lowest being 0.10m (several stations in the North Sea) and the highest being 0.49m (Oudeschild in the Wadden Sea). These errors are higher than the expected vertical accuracy, but it is expected that for the open ocean, the error values will decrease. The amount of 'good quality' datapoints steeply increases with increasing distance from the coast, which will improve the quality of the fit. This was also found by Kupavõh et al. (2025), where they found a great improvement of valid datapoints from SWOT near the coast compared to previous satellite altimetry missions. The improved spatial resolution has a great contribution to his. From other satellite altimetry missions, it is known that the performance near the coast causes problems (Vignudelli et al., 2019). Land contamination makes it difficult to interpret the complex returned radar signal. The choice of coordinate for the SWOT measurement does affect the found correlation for a specific tidal gauge station on the coastline. Often, the results are improved if you choose a coordinate further from the coast. However, the measurements are still not as accurate as in the deep ocean. Several factors contribute to this, such as the decrease in the ability to accurately determine correction factors in coastal areas. In the case where a coordinate further seaward was chosen for the validation of the SWOT data at Brouwershavense Gat 8, a significant increase in R^2 value is observed, along with a decrease in the RMSE. However, also the bias decreased from -0.09 cm to -0.01 cm. This raises caution, since it was found that the bias is relatively constant to be around 10 cm. The choice of a coordinate further offshore could impact the results of SSH measurements due to coastal setup, a rise in sea level near the shore caused by tidal forcing, wind stress, and bathymetric effects. Consequently, choosing other coordinates for validation might introduce systematic differences in SSH, even over short distances, potentially leading to apparent discrepancies between in-situ data and satellite observations.

The effects of the intertidal environment in the Wadden Sea become apparent from the scatter plots. They show distinct differences between measurements taken during high and low tide. During high tide (SSH > 0m) there appears to be less scatter then during low tide (SSH < 0m). Exposed sandbanks, which cause land contamination are the likely cause for this effect in the specific area of the Wadden Sea. Salameh et al. (2021) has looked at the potential for SWOT to monitor intertidal topography using its higher spatial resolution and 2D wide swath SSH results. In the Bay of Veys, a shallow

estuarine embayment, this has been successfully tried using the data from the Cal/Val phase (Salameh et al., 2024). Using SWOT observations, they obtained a mean absolute error lower than 0.49m, which is considered a good value for coastal applications. It would be interesting to study if this could benefit the application of SWOT to measure the water surface heights in complex intertidal environments such as the Wadden Sea.

The main differences between the different environments are that the amount of 'good quality' datapoints is substantially lower in the Wadden Sea and close to the coast and that the RMSE is higher in the Wadden Sea. This consequently impacts the accuracy of the harmonic analysis. The lower quality of SSH observations in the Wadden Sea results in higher RMSE and less reliable harmonic fits. This affects both the M_2 and M_4 components, particularly M_4, which is more sensitive to noise due to its smaller amplitude. The M_4 amplitude is generally lower than 0.30m, which thus is in the same order of magnitude as the observed RMSE in the Wadden Sea, and also close to the RMSE in the North Sea. Contrary, the M_2 tidal amplitude is generally around 2m, which would thus be less sensitive to noise. Consequently, tidal parameters derived from SWOT in the Wadden Sea, and other complex regions should be interpreted with caution, while results over the North Sea are expected to be more representative.

The vertical accuracy of SWOT SSH measurements is comparable to previous satellite altimetry missions (e.g. Dettmering et al., 2021; Madsen et al., 2007; Rulent et al., 2020) The expected vertical accuracy for SWOT falls within the same range as that of missions such as TOPEX/Poseidon, the Jason series, and Sentinel, all of which report vertical accuracies between 5 and 10 cm. For example, Madsen et al. (2007) reported correlations exceeding 90% between tide gauge data and nearby altimetry observations from TOPEX/Poseidon and Jason-1. When excluding tide gauge stations in the Wadden Sea, the average correlation between SWOT SSH measurements and stations in the North Sea reaches 0.94. Similarly, Dettmering et al. (2021) found a mean correlation of 0.85 between multi-mission altimetry and tide gauge observations, consistent with the findings of Madsen. Dettmering also calculated the RMSE of satellite altimetry relative to tide gauge data, reporting median RMSE values between 3 and 8 cm, comparable to the 6 cm RMSE found for the North Sea stations in this study. However, whereas the present study used the nearest satellite grid point for comparison, Dettmering selected the 20% best-correlated gridded altimetry observations within a 200 km radius of each tide gauge station. This method tends to enhance the agreement between datasets (Oelsmann et al., 2021).

Overall, SWOT is expected to offer the most significant advancements in complex coastal regions, where previous satellite altimetry missions lacked the spatial resolution necessary for accurate SSH measurements.

4.2 Harmonic analysis in the North Sea

The spatial distribution of the tidal characteristics from SWOT data provides to a certain extent a physically consistent representation of the dominant tidal dynamics in the North Sea. However, there is a difference between the results for the M_2 and M_4 tidal constituent. First, the results for the M_2 constituent are discussed. The observed pattern of larger tidal amplitudes along the coast and in constricted regions such as the English Channel align with expectations of semi-enclosed shelf seas. It also captures the occurrence of two amphidromic points that are known in the North Sea (Roos & De Swart, 2022). The SNR for the M_2 tides indicate a strong fit as well, with values generally above 10^6. However, there are certain areas where the SNR is lower, such as near the amphidromic points, where the SNR is near zero. Certain passes (e.g. pass 542) show a lower SNR (below 10^4), indicating that the individual measurements could also influence the performance of the harmonic analysis.

Extreme or episodic events captured by SWOT during certain passes can introduce variability between passes. Additionally, in the nadir of the swot passes, there is a reduction of the SNR visible. This might be because of the reduction of datapoints at these locations, because of the lack of measurements of the wide swath at the nadir. The M_4 tidal constituent appears to be less accurate with the harmonic analysis. It does show that the amplitude of the M_4 tide is largest in shallow regions near the coast and less significant in the deeper parts of the North Sea. However, there seems to be more differences between different passes and more noise in the reconstruction. This is also reflected in the lower SNR ($<10^3$), with several areas in the range of 0.01-0.1, indicating that the results are unreliable due to the amount of noise in the harmonic analysis. This can be explained by the amplitude of the M_4 tide and the RMSE of SSH measurements by SWOT. The RMSE (0.22m average, 0.14m in open sea) is in the same range as the expected values for the M_4 tidal amplitude (0-0.3m). Hence it is very likely that the M_4 tidal constituent in this reconstruction is deluded because of the error in SSH measurements. The M_2 tidal amplitude is generally higher in the North Sea ($\sim$2m), which means that the error in SWOT SSH measurements does not impact the results of the harmonic analysis to the same extent as for the M_4 tidal constituent.

In this thesis, the reconstruction of the tidal signal has been done using a representative tidal signal. Due to the irregular temporal distribution of SWOT observations, tidal reconstruction for a single tidal cycle is performed by referencing each measurement to the most recent local high-water event. While this method allows for consistent alignment of semidiurnal signals (e.g. M_2), it becomes problematic for constituents with lower frequencies, such as diurnal (e.g. K_1, O_1) and long-period tides (e.g. M_m, S_a). These constituents vary more slowly and cannot be adequately resolved using relative timing within a single semidiurnal cycle. As a result, their influence may distort the reconstructed semidiurnal signal and complicates the spectral separation of tidal components.

Additionally, to reduce the influence of outliers caused by the irregular sampling of SWOT within the spring-neap cycle, all SSH measurements were normalised by the local spring tidal range. This correction effectively scales all observations to represent spring tide conditions. As a consequence, the resulting harmonic analysis no longer resolves individual constituents like M_2 and S_2 independently. Instead, it captures a combined signal that reflects the amplitude modulation of the spring-neap cycle, which is governed by the interference between M_2 and S_2. Therefore, the estimated M_2 amplitude includes contributions from both M_2 and S_2, potentially biasing the interpretation of the constituent's strength.

In contrast to the representative tidal cycle method used in this thesis, Hart-Davis et al. (2024) applied a tidal aliasing technique based on SWOT Cal/Val data (see section 1.4). Their method relies on the regular aliasing of tidal signals, allowing for independent estimation of multiple constituents, provided the alias frequencies remain well separated and the SNR is sufficient. Although the method developed in this thesis allows for consistent spatial mapping of the dominant tide (M_2), it lacks the frequency resolution required to separate tidal constituents of lower frequencies. Thus, unlike the aliasing method, the present approach does not resolve tidal components independently but instead provides a robust estimate of the dominant tidal behaviour under sparse sampling constraints. So, the representative tidal cycle method is suited for situations with irregular or sparse temporal sampling, where the assumptions underlying tidal aliasing may be less applicable. However, this method requires a continuous, accurate, and high frequency reference for SSH measurements, such as a tidal gauge station available in the area.

Satellite altimetry data has been used before to analyse the tidal signal (e.g. Egbert & Ray, 2001; Ray & Zaron, 2016). The main limitations always were the temporal and spatial undersampling of those satellites. The combination of multi-satellite data markedly improves spatial coverage by combining

the track coverages of those datasets (Zhao et al., 2011). The traditional altimeter only provides measurements at the nadir, so spatial integration is needed for most purposes. The SWOT mission can overcome those limitations using the wide swath data it provides. Consequently, the results of the tidal analysis will improve as well.

5. Conclusion

The study aimed to validate the SWOT measurements in the Dutch coastal environment and to reconstruct the semidiurnal tidal signal of the North Sea based on SWOT data.

The correlation between SWOT SSH measurements and tidal gauge stations is good (R^2 = 0.88) and a RMSE of 0.22m. There is, however, a persistent bias of -0.14 m, indicating an overestimation of the SSH by SWOT. Between the three indicated regions, differences are noted, which relate to land contamination effects and the spatial resolution. Near the coastal tidal gauge stations, only 6.3% of the SWOT data was qualified as 'good quality', in contrast to 48% for the stations located further in the North Sea. In the Wadden Sea, an intertidal area, the accuracy degraded further, with a reduced correlation (R^2 = 0.79) and a higher RMSE of 0.34 m. The proportion of good quality observations dropped significantly to just 0.79%. This decline in performance can be attributed to the complex topography, shallow water depth, and increased land contamination in SWOT's radar signal. There is a difference visible between high and low water levels, suggesting the accuracy is better during high tide. While the overall performance remains strong offshore, these results highlight the current limitations of SWOT Low Resolution oceanography data in highly dynamic coastal environments such as the Wadden Sea. Future work should explore the use of SWOT's High-Rate hydrology datasets to improve the performance in areas such as the Wadden Sea.

Secondly, a method to reconstruct the tidal signal in the North Sea was introduced by using a representative tidal cycle. For this, SWOT measurements scaled for the spring-neap cycle were used. The resulting M_2 and M_4 tidal signals reproduce known tidal features in the region. However, there are some limitations in using this approach. Since the RMSE is in the same range as the M_4 amplitude (0-0.3m), the resulting fit is less strong than that of the M_2 tide, which has a larger amplitude. Additionally, by fitting the data in one representative tidal signal, low frequency tidal signals are lost in the process and subsequently impact the resolved signal of other constituents. Furthermore, this method essentially fits the dominant semidiurnal signal, which is a mix of the M_2 and S_2 constituent, since it corrects all SWOT measurements to spring tidal range. Compared to the more common method of tidal aliasing, this approach cannot resolve the tidal components independently as good. However, it is better suited for situations where the temporal resolution is coarse or data availability is limited, and tidal aliasing techniques become less effective.

In summary, this research advances our understanding of SWOT and radar interferometry for SSH and tidal applications. Highlighting both its promises in open ocean and the challenges remaining in near-shore and intertidal environments.

References

CNES (n.d. a). *GPSP TRACKING RECIEVER.* AVISO+. Visited on 16 May 2025. *https://www.aviso.altimetry.fr/en/missions/current-missions/jason-3/instruments/gpsp*

CNES (n.d. b). *LRA: Laser Retroflector Array.* AVISO+. Visited on 16 May 2025. https://www.aviso.altimetry.fr/en/missions/current-missions/saral/instruments-1/lra

CNES (n.d. c). *SWOT KaRIn Low Rate Ocean Products.* AVISO+. Visited on 16 May 2025. https://www.aviso.altimetry.fr/en/data/products/sea-surface-height-products/global/swot-karin-low-rate-ocean-products.html

Chelton, D. B., DeSzoeke, R. A., Schlax, M. G., El Naggar, K., & Siwertz, N. (1998). Geographical variability of the first baroclinic Rossby radius of deformation. *Journal of Physical Oceanography*, *28*(3), 433-460.

Chelton, D. B., Ries, J. C., Haines, B. J., Fu, L. L., & Callahan, P. S. (2001). *Chapter 1 Satellite Altimetry. Satellite Altimetry and Earth Sciences - A Handbook of Techniques and Applications, (pp. 1-131, i-ii). Academic Press.* https://doi.org//10.1016/s0074-6142(01)80146-7

Codiga, D. L. (2011). Unified tidal analysis and prediction using the UTide Matlab functions. Technical report 2011-01. Graduate School of Oceanography, University of Rhode Island, Narragansett, RI. https://dx.doi.org/10.13140/RG.2.1.3761.2008

Dettmering, D., Müller, F. L., Oelsmann, J., Passaro, M., Schwatke, C., Restano, M., ... & Seitz, F. (2021). North SEAL: a new dataset of sea level changes in the North Sea from satellite altimetry. *Earth System Science Data*, *13*(8), 3733-3753.

Egbert, G. D., & Ray, R. D. (2001). Estimates of M2 tidal energy dissipation from TOPEX/Poseidon altimeter data. *Journal of Geophysical Research: Oceans*, *106*(C10), 22475-22502.

Fu, L. L., & Cazenave, A. (Eds.). (2000). *Satellite altimetry and earth sciences: a handbook of techniques and applications* (Vol. 69). Elsevier. https://doi.org/10.1016/s0074-6142 (01)x8144-8

Fu, L. L., & Le Traon, P. Y. (2006). Satellite altimetry and ocean dynamics. *Comptes Rendus Geoscience*, *338*(14-15), 1063-1076. https://doi.org/10.1016/j.crte.2006.05.015

Fu, L. L., Alsdorf, D., Morrow, R., Rodriguez, E., & Mognard, N. (2012). *SWOT: The surface water and ocean topography mission. Wide-swath altimetric elevation on Earth* (Version 2.0). Pasadena, CA: Jet Propulsion Laboratory, National Aeronautics and Space Administration. DOI: 2014/41996.

Fu, L.L., & Rodriguez, E. (2004). *High-resolution measurement of ocean surface topography by radar interferometry for oceanographic and geophysical applications.* In R. S. J. Sparks, C.J. Hawkesworth (Eds.), *The state of the planet: Frontiers and challenges in geophysics* (pp. 209–224). American Geophysical Union. https://doi.org/10.1029/150GM17

Hart-Davis, M. G., Andersen, O. B., Ray, R. D., Zaron, E. D., Schwatke, C., Arildsen, R. L., ... & Nielsen, K. (2024). Tides in complex coastal regions: Early case studies from wide-swath SWOT measurements. *Geophysical Research Letters*, *51*(20), e2024GL109983.

Hart-Davis, M. G., Piccioni, G., Dettmering, D., Schwatke, C., Passaro, M., & Seitz, F. (2021). EOT20: A global ocean tide model from multi-mission satellite altimetry. *Earth System Science Data*, *13*(8), 3869-3884. https://doi.org/10.5194/essd-13-3869-2021

Hydrographic Service Ministry of Defence. (2020). *NLLAT2018: New vertical reference surface for the North Sea*. Retrieved from https://english.defensie.nl/downloads/applications/2020/06/12/nllat2018

Intergovernmental Oceanographic Commission (2006). *Manual on sea level measurement and interpretation. Volume IV: An Update to 2006*. Paris, France: UNESCO. https://doi.org/10.25607/OBP-1398

NASA, Jet Propulsion Laboratory (n.d.). *Science Overview. SWOT – Surface Water and Ocean Topography*. Visited on 16 May 2025, from https://swot.jpl.nasa.gov/science/overview/

JPL D-109532, Revision A, "SWOT Science Data Products User Handbook," Jet Propulsion Laboratory Internal Document, Pasadena, CA, 2025. Retrieved from https://podaac.jpl.nasa.gov/SWOT?tab=datasets-information&sections=about%2Bdata%2Bresources

Kupavõh, A., Delpeche-Ellmann, N., Ellmann, A., & Soomere, T. (2025). Examining the Performance of Satellite Altimetry (SWOT) Sea Level Data in the Coastal Areas of the Baltic Sea. *Journal of Coastal Research*, *113*(SI), 534-538. https://doi.org/10.2112/JCR-SI113-105.1

Madsen, K. S., Høyer, J. L., & Tscherning, C. C. (2007). Near-coastal satellite altimetry: Sea surface height variability in the North Sea–Baltic Sea area. *Geophysical Research Letters*, *34*(14).

Matthäus, W. (1972). On the History of Recording Tide Gauges. *Proceedings Of The Royal Society Of Edinburgh Section B Biological Sciences*, *73*, 26–34. https://doi.org/10.1017/s0080455x00002083

Merrifield, M. A., Merrifield, S. T., & Mitchum, G. T. (2009). An anomalous recent acceleration of global sea level rise. *Journal of Climate*, *22*(21), 5772-5781. https://doi.org/10.1175/2009JCLI2985.1

NASA Earthdata (n.d.). *DORIS.* Visited on 16 May 2025, from https://www.earthdata.nasa.gov/data/space-geodesy-techniques/doris

NASA PODAAC. (2023). *SWOT Level 2 Science Data Products User Guide*. https://podaac.jpl.nasa.gov/dataset/SWOT_L2_LR_SSH_2.0

Oelsmann, J., Passaro, M., Dettmering, D., Schwatke, C., Sánchez, L., & Seitz, F. (2021). The zone of influence: matching sea level variability from coastal altimetry and tide gauges for vertical land motion estimation. *Ocean Science*, *17*(1), 35-57.

Parker, B.B. (2007) Tidal analysis and prediction. Silver Spring, MD, NOAA NOS Center for Operational Oceanographic Products and Services, 378pp (NOAA Special Publication NOS CO-OPS 3). DOI: http://dx.doi.org/10.25607/OBP-191

Pugh, D. T. (1996). Tides, surges and mean sea-level (reprinted with corrections). *John Wiley & Sons.* https://eprints.soton.ac.uk/19157/

Pugh, D. T. (1987). Tides, surges and mean sea level. John Wiley & Sons.

Ray, R. D. (2013). Precise comparisons of bottom-pressure and altimetric ocean tides. *Journal of Geophysical Research: Oceans*, *118*(9), 4570-4584. https://doi.org/10.1002/jgrc.20336

Ray, R. D., & Zaron, E. D. (2016). M 2 internal tides and their observed wavenumber spectra from satellite altimetry. *Journal of Physical Oceanography*, *46*(1), 3-22.

Rijkswaterstaat. (2010). *De Rijkswaterstaat standaard voor de inwinning, verwerking en uitgifte van hydrologische en meteorologische gegevens* (Versie 2.2). Ministerie van Verkeer en Waterstaat, Directoraat-Generaal Rijkswaterstaat.

Rodriguez, E., & Martin, J. M. (1992). *Theory and design of interferometric synthetic aperture radars. IEE Proceedings F (Radar and Signal Processing), 139(2), 147-159.* doi:10.1049/ip-f-2.1992.0018

Roos, P. C., & De Swart, H. E. (2022). Tides in Coastal Seas. Influence of Topography and Bottom Friction. In *The Mathematics of Marine Modelling: Water, Solute and Particle Dynamics in Estuaries and Shallow Seas* (pp. 73-102). Cham: Springer International Publishing. https://doi.org/10.1007/978-3-031-09559-7_4

Rulent, J., Calafat, F. M., Banks, C. J., Bricheno, L. M., Gommenginger, C., Green, J. M., ... & Martin, A. C. (2020). Comparing water level estimation in coastal and shelf seas from satellite altimetry and numerical models. *Frontiers in Marine Science*, *7*, 549467. https://doi.org/10.1016/j.rse.2024.114401

Salameh, E., Desroches, D., Deloffre, J., Fjørtoft, R., Mendoza, E. T., Turki, I., ... & Frappart, F. (2024). Evaluating SWOT's interferometric capabilities for mapping intertidal topography. *Remote Sensing of Environment*, *314*, 114401. https://doi.org/10.1016/j.rse.2024.114401

Salameh, E., Frappart, F., Desroches, D., Turki, I., Carbonne, D., & Laignel, B. (2021). Monitoring intertidal topography using the future SWOT (Surface Water and Ocean Topography) mission. *Remote Sensing Applications: Society and Environment*, *23*, 100578. https://doi.org/10.1016/j.rsase.2021.100578

Stammer, D., Ray, R. D., Andersen, O. B., Arbic, B. K., Bosch, W., Carrere, L., ... & Yi, Y. (2014). Accuracy assessment of global barotropic ocean tide models. *Reviews of geophysics*, *52*(3), 243-282. https://doi.org/10.1002/2014RG000450

Surface Water Ocean Topography (SWOT). (2023). *SWOT product description L2_LR_SSH_20220902 RevA.* https://archive.podaac.earthdata.nasa.gov/podaac-ops-cumulus-docs/web-misc/swot_mission_docs/pdd/D-56407_SWOT_Product_Description_L2_LR_SSH_20220902_RevA.pdf

Surface Water Ocean Topography (SWOT). 2024. SWOT Level 2 KaRIn Low Rate Sea Surface Height Data Product - Expert, Version C. Ver. C. PO.DAAC, CA, USA. Dataset accessed [2025-03-18] at https://doi.org/10.5067/SWOT-SSH-2.0

SWOT Project. (2024, October 14). *Surface Water and Ocean Topography (SWOT) Project: Release Note Version C KaRIn Science Data Products.* NASA Jet Propulsion Labaratory/CNES. Retrieved from https://www.aviso.altimetry.fr/fileadmin/documents/data/tools/SWOT_VersionC_KaRIn_Products_Release_Note_20241014.pdf

Vignudelli, S., Birol, F., Benveniste, J. *et al.* Satellite Altimetry Measurements of Sea Level in the Coastal Zone. *Surv Geophys* 40, 1319–1349 (2019). https://doi.org/10.1007/s10712-019-09569-1

Volkov, D. L. (2004). *Monitoring the variability of sea level and surface circulation with satellite altimetry*. Utrecht University. https://dspace.library.uu.nl/bitstream/1874/1105/9/full.pdf

Volkov, D. L., Larnicol, G., & Dorandeu, J. (2007). Improving the quality of satellite altimetry data over continental shelves. *Journal of Geophysical Research: Oceans*, *112*(C6).

Zhao, Z., M. H. Alford, J. Girton, T. S. Johnston, and G. Carter, 2011*:* Internal tides around the Hawaiian Ridge estimated from multisatellite altimetry*. J. Geophys. Res.*, *116*, C12039, doi:10.1029/2011JC007045.

Appendix A: Location of tidal gauge stations

North Sea stations:

Station	*Longitude (°)*	*Latitude (°)*
Vlakte van de Raan	3.2	51.5
Wierumergronden	6.0	53.5
Oosterschelde 11	3.5	51.6
Lichteiland Goeree	3.7	51.9
K13a platform	3.2	53.2
Huibertgat	6.4	53.6
Haringvliet 10	3.9	51.9
Europlatform	3.3	52.0
Brouwershavense Gat 2	3.6	51.8

Coastal stations:

Station	*Longitude (°)*	*Latitude (°)*
Berghaven H v Holland	4.1	52.0
Brouwershavensche Gat 8	3.8	51.8
Cadzand	3.4	51.4
Den Helder	4.7	53.0
Hoek van Holland	4.1	52.0
Hollandse kust noord	4.6	52.8
IJgeul stroommeetpaal	4.5	52.5
Oosterschelde 4	3.7	51.7
Scheveningen	4.2	52.1
Stellendam buiten	4.0	51.8
Terschelling Noordzee	5.3	53.4
Texel Noordzee	4.8	53.1
Vlissingen	3.6	51.4
Westkapelle	3.4	51.5

Wadden Sea stations:

Station	*Longitude (°)*	*Latitude (°)*
Den Helder Veersteiger 2	4.8	53.0
Den Oever buiten	5.0	52.9
Harlingen	5.4	53.2
Kornwerderzand buiten zui	5.3	53.1
Lauwersoog	6.2	53.4
Nes	5.8	53.4
Oudeschild	4.9	53.0
Schiermonnikoog	6.2	53.5
Stroommeetpaal Eemshaven	6.8	53.5
Uithuizerwad 2	6.8	53.5
Vlieland haven	5.1	53.3
West-Terschelling	5.2	53.4

Appendix B: Validation tidal gauge stations Rijkswaterstaat

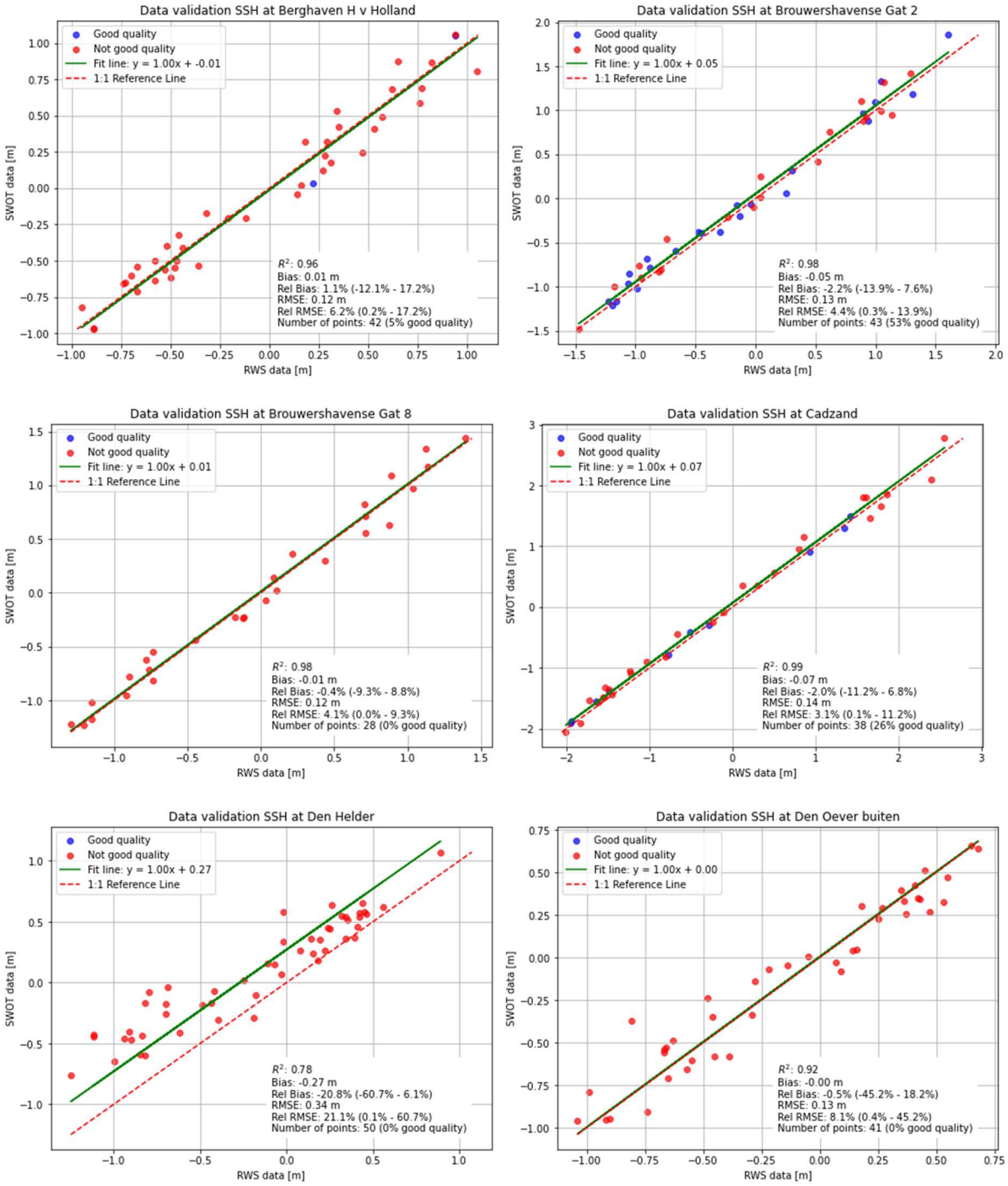

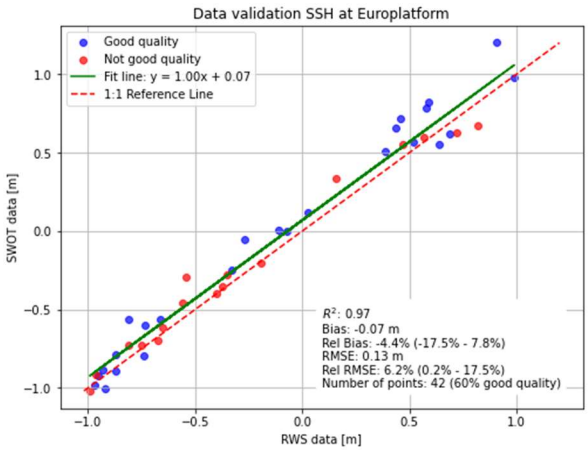
Data validation SSH at Europlatform
Good quality
Not good quality
Fit line: y = 1.00x + 0.07
1:1 Reference Line
R^2: 0.97
Bias: -0.07 m
Rel Bias: -4.4% (-17.5% - 7.8%)
RMSE: 0.13 m
Rel RMSE: 6.2% (0.2% - 17.5%)
Number of points: 42 (60% good quality)
SWOT data [m]
RWS data [m]

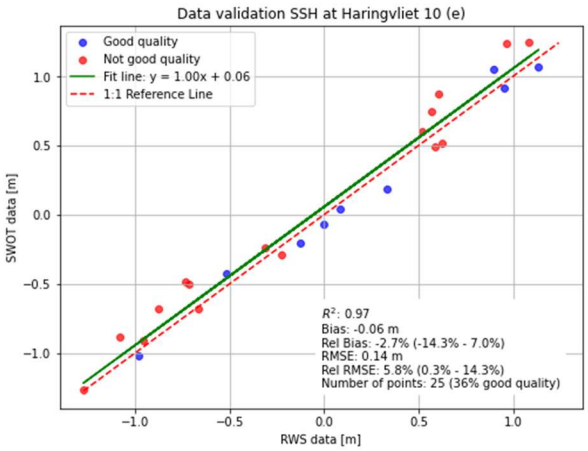
Data validation SSH at Haringvliet 10 (e)
Good quality
Not good quality
Fit line: y = 1.00x + 0.06
1:1 Reference Line
R^2: 0.97
Bias: -0.06 m
Rel Bias: -2.7% (-14.3% - 7.0%)
RMSE: 0.14 m
Rel RMSE: 5.8% (0.3% - 14.3%)
Number of points: 25 (36% good quality)
SWOT data [m]
RWS data [m]

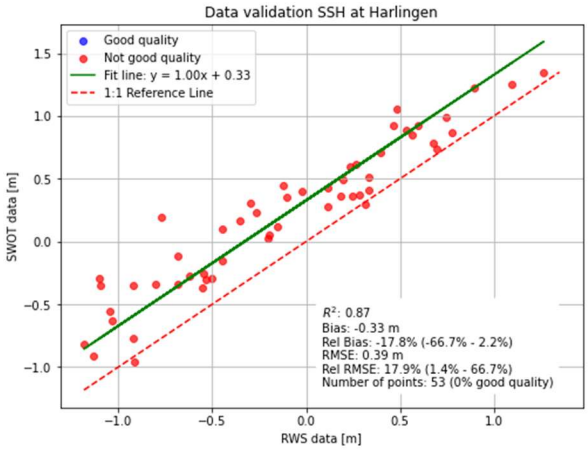
Data validation SSH at Harlingen
Good quality
Not good quality
Fit line: y = 1.00x + 0.33
1:1 Reference Line
R^2: 0.87
Bias: -0.33 m
Rel Bias: -17.8% (-66.7% - 2.2%)
RMSE: 0.39 m
Rel RMSE: 17.9% (1.4% - 66.7%)
Number of points: 53 (0% good quality)
SWOT data [m]
RWS data [m]

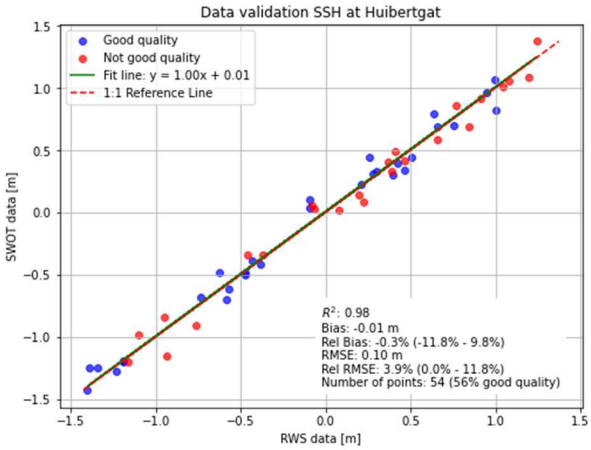
Data validation SSH at Huibertgat
Good quality
Not good quality
Fit line: y = 1.00x + 0.01
1:1 Reference Line
R^2: 0.98
Bias: -0.01 m
Rel Bias: -0.3% (-11.8% - 9.8%)
RMSE: 0.10 m
Rel RMSE: 3.9% (0.0% - 11.8%)
Number of points: 54 (56% good quality)
SWOT data [m]
RWS data [m]

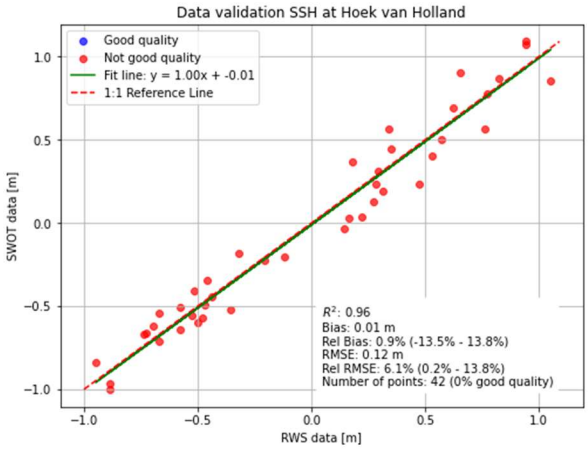
Data validation SSH at Hoek van Holland
Good quality
Not good quality
Fit line: y = 1.00x + -0.01
1:1 Reference Line
R^2: 0.96
Bias: 0.01 m
Rel Bias: 0.9% (-13.5% - 13.8%)
RMSE: 0.12 m
Rel RMSE: 6.1% (0.2% - 13.8%)
Number of points: 42 (0% good quality)
SWOT data [m]
RWS data [m]

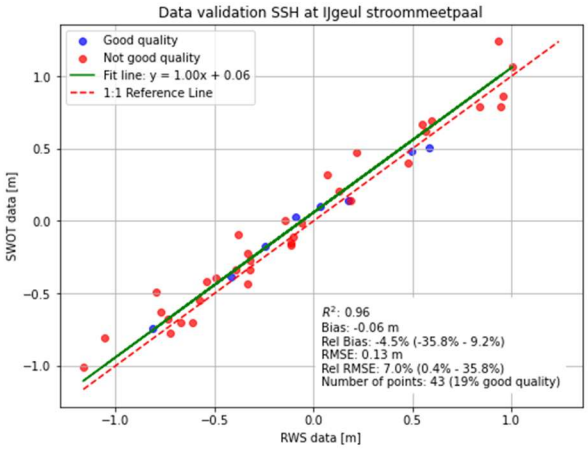
Data validation SSH at IJgeul stroommeetpaal
Good quality
Not good quality
Fit line: y = 1.00x + 0.06
1:1 Reference Line
R^2: 0.96
Bias: -0.06 m
Rel Bias: -4.5% (-35.8% - 9.2%)
RMSE: 0.13 m
Rel RMSE: 7.0% (0.4% - 35.8%)
Number of points: 43 (19% good quality)
SWOT data [m]
RWS data [m]

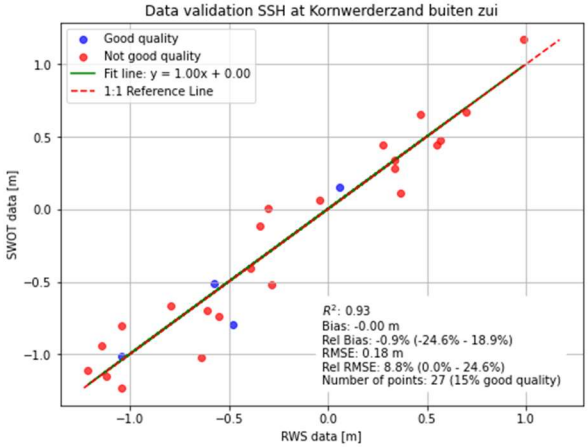
Data validation SSH at Kornwerderzand buiten zui
Good quality
Not good quality
Fit line: y = 1.00x + 0.00
1:1 Reference Line
R^2: 0.93
Bias: -0.00 m
Rel Bias: -0.9% (-24.6% - 18.9%)
RMSE: 0.18 m
Rel RMSE: 8.8% (0.0% - 24.6%)
Number of points: 27 (15% good quality)
SWOT data [m]
RWS data [m]

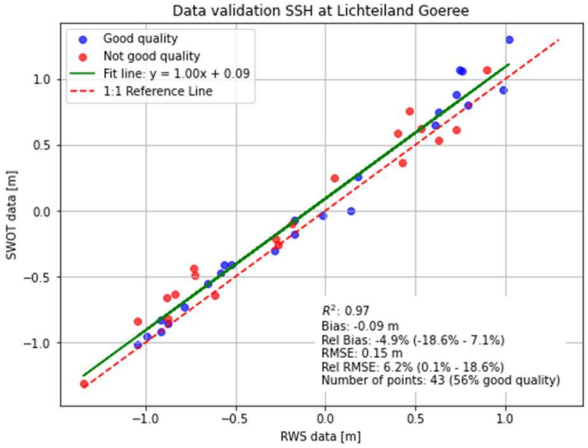
Data validation SSH at Lichteiland Goeree
Good quality
Not good quality
Fit line: y = 1.00x + 0.09
1:1 Reference Line
R^2: 0.97
Bias: -0.09 m
Rel Bias: -4.9% (-18.6% - 7.1%)
RMSE: 0.15 m
Rel RMSE: 6.2% (0.1% - 18.6%)
Number of points: 43 (56% good quality)
SWOT data [m]
RWS data [m]

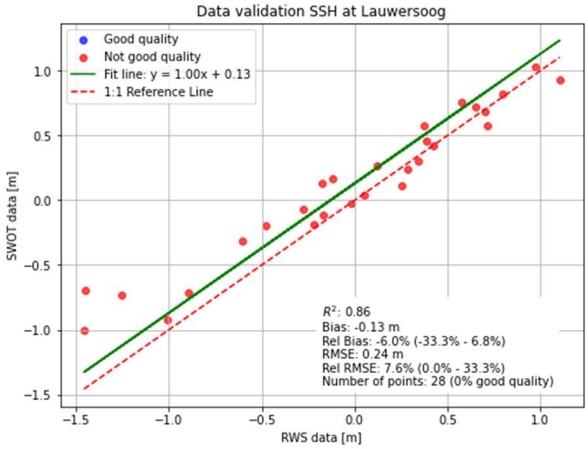
Data validation SSH at Lauwersoog
Good quality
Not good quality
Fit line: y = 1.00x + 0.13
1:1 Reference Line
R^2: 0.86
Bias: -0.13 m
Rel Bias: -6.0% (-33.3% - 6.8%)
RMSE: 0.24 m
Rel RMSE: 7.6% (0.0% - 33.3%)
Number of points: 28 (0% good quality)
SWOT data [m]
RWS data [m]

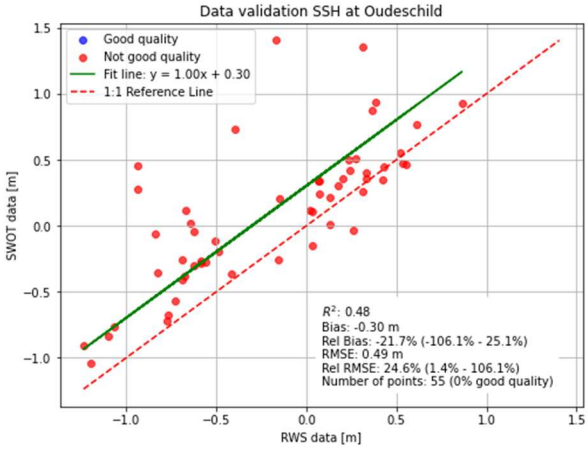
Data validation SSH at Oudeschild
Good quality
Not good quality
Fit line: y = 1.00x + 0.30
1:1 Reference Line
R^2: 0.48
Bias: -0.30 m
Rel Bias: -21.7% (-106.1% - 25.1%)
RMSE: 0.49 m
Rel RMSE: 24.6% (1.4% - 106.1%)
Number of points: 55 (0% good quality)
SWOT data [m]
RWS data [m]

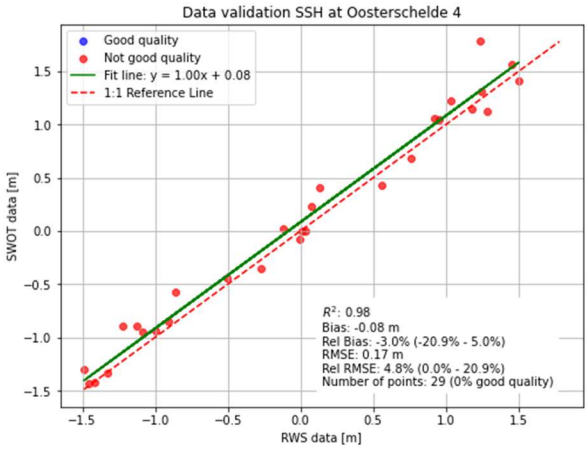
Data validation SSH at Oosterschelde 4
Good quality
Not good quality
Fit line: y = 1.00x + 0.08
1:1 Reference Line
R^2: 0.98
Bias: -0.08 m
Rel Bias: -3.0% (-20.9% - 5.0%)
RMSE: 0.17 m
Rel RMSE: 4.8% (0.0% - 20.9%)
Number of points: 29 (0% good quality)
SWOT data [m]
RWS data [m]

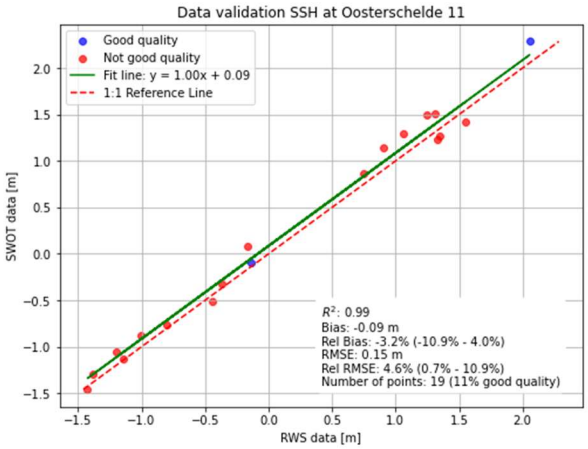
Data validation SSH at Oosterschelde 11
Good quality
Not good quality
Fit line: y = 1.00x + 0.09
1:1 Reference Line
R^2: 0.99
Bias: -0.09 m
Rel Bias: -3.2% (-10.9% - 4.0%)
RMSE: 0.15 m
Rel RMSE: 4.6% (0.7% - 10.9%)
Number of points: 19 (11% good quality)
SWOT data [m]
RWS data [m]

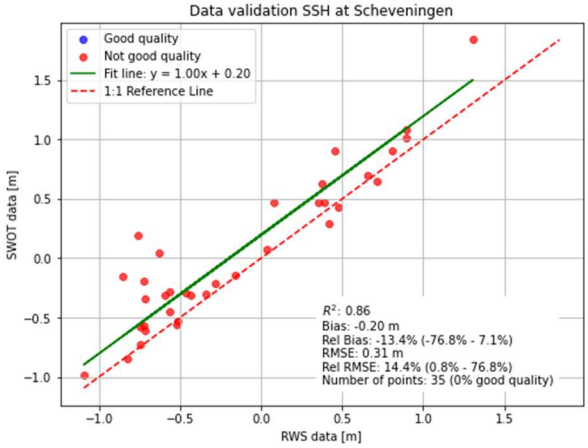
Data validation SSH at Scheveningen
Good quality
Not good quality
Fit line: y = 1.00x + 0.20
1:1 Reference Line
R^2: 0.86
Bias: -0.20 m
Rel Bias: -13.4% (-76.8% - 7.1%)
RMSE: 0.31 m
Rel RMSE: 14.4% (0.8% - 76.8%)
Number of points: 35 (0% good quality)
SWOT data [m]
RWS data [m]

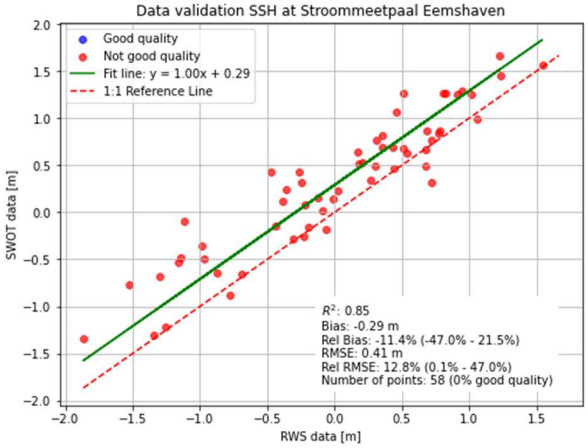
Data validation SSH at Stroommeetpaal Eemshaven
Good quality
Not good quality
Fit line: y = 1.00x + 0.29
1:1 Reference Line
R^2: 0.85
Bias: -0.29 m
Rel Bias: -11.4% (-47.0% - 21.5%)
RMSE: 0.41 m
Rel RMSE: 12.8% (0.1% - 47.0%)
Number of points: 58 (0% good quality)
SWOT data [m]
RWS data [m]

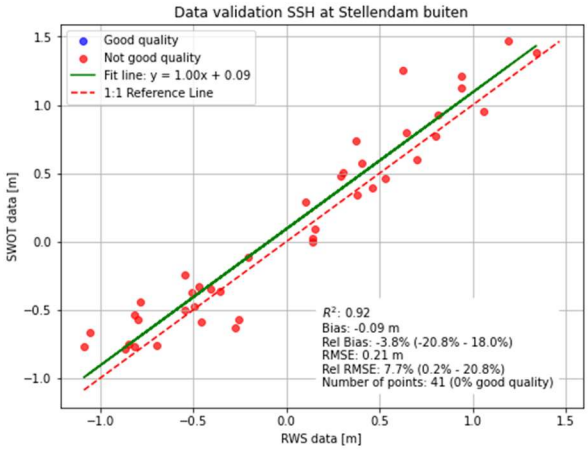
Data validation SSH at Stellendam buiten
Good quality
Not good quality
Fit line: y = 1.00x + 0.09
1:1 Reference Line
R^2: 0.92
Bias: -0.09 m
Rel Bias: -3.8% (-20.8% - 18.0%)
RMSE: 0.21 m
Rel RMSE: 7.7% (0.2% - 20.8%)
Number of points: 41 (0% good quality)
SWOT data [m]
RWS data [m]

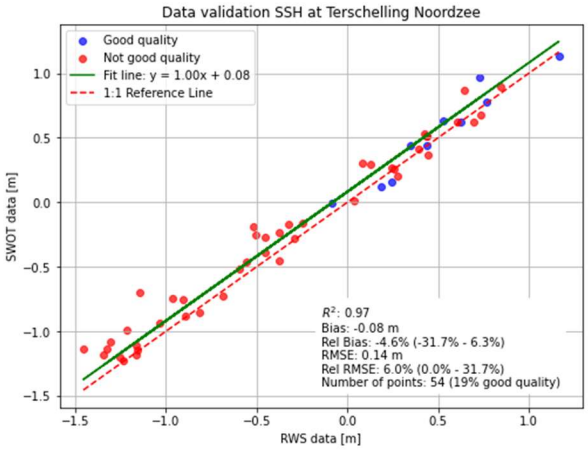
Data validation SSH at Terschelling Noordzee
Good quality
Not good quality
Fit line: y = 1.00x + 0.08
1:1 Reference Line
R^2: 0.97
Bias: -0.08 m
Rel Bias: -4.6% (-31.7% - 6.3%)
RMSE: 0.14 m
Rel RMSE: 6.0% (0.0% - 31.7%)
Number of points: 54 (19% good quality)
SWOT data [m]
RWS data [m]

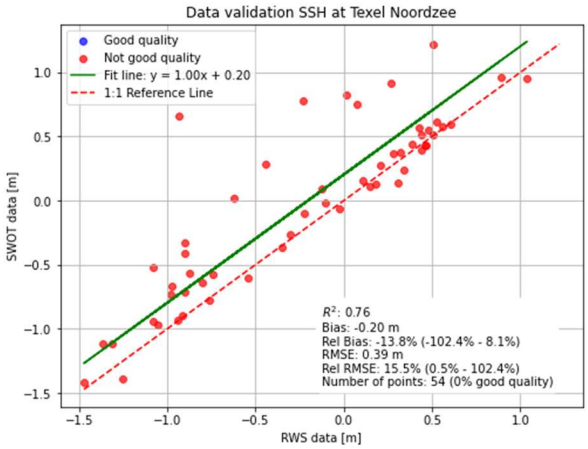
Data validation SSH at Texel Noordzee
Good quality
Not good quality
Fit line: y = 1.00x + 0.20
1:1 Reference Line
R^2: 0.76
Bias: -0.20 m
Rel Bias: -13.8% (-102.4% - 8.1%)
RMSE: 0.39 m
Rel RMSE: 15.5% (0.5% - 102.4%)
Number of points: 54 (0% good quality)
SWOT data [m]
RWS data [m]

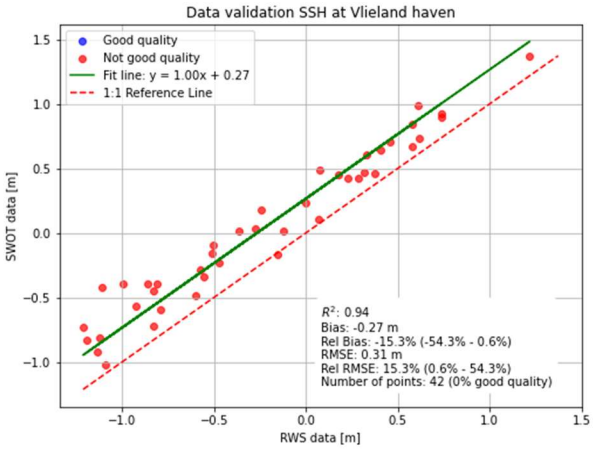
Data validation SSH at Vlieland haven
Good quality
Not good quality
Fit line: y = 1.00x + 0.27
1:1 Reference Line
R^2: 0.94
Bias: -0.27 m
Rel Bias: -15.3% (-54.3% - 0.6%)
RMSE: 0.31 m
Rel RMSE: 15.3% (0.6% - 54.3%)
Number of points: 42 (0% good quality)
SWOT data [m]
RWS data [m]

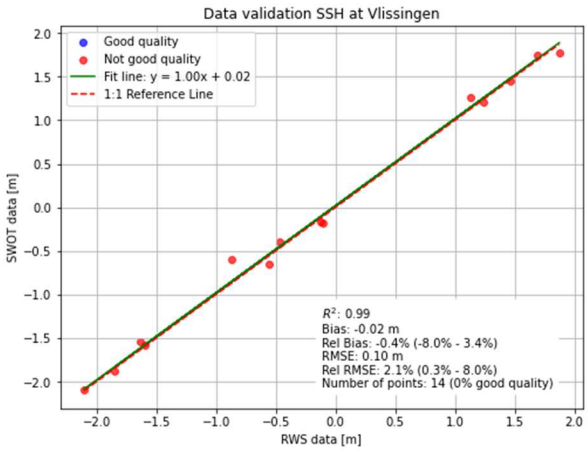
Data validation SSH at Vlissingen
Good quality
Not good quality
Fit line: y = 1.00x + 0.02
1:1 Reference Line
R^2: 0.99
Bias: -0.02 m
Rel Bias: -0.4% (-8.0% - 3.4%)
RMSE: 0.10 m
Rel RMSE: 2.1% (0.3% - 8.0%)
Number of points: 14 (0% good quality)
SWOT data [m]
RWS data [m]

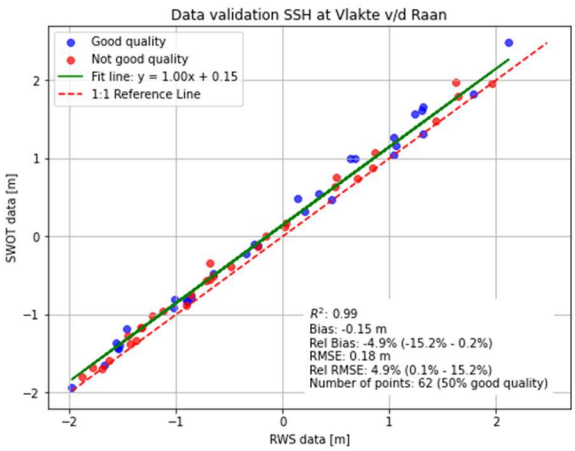
Data validation SSH at Vlakte v/d Raan
Good quality
Not good quality
Fit line: y = 1.00x + 0.15
1:1 Reference Line
R^2: 0.99
Bias: -0.15 m
Rel Bias: -4.9% (-15.2% - 0.2%)
RMSE: 0.18 m
Rel RMSE: 4.9% (0.1% - 15.2%)
Number of points: 62 (50% good quality)
SWOT data [m]
RWS data [m]

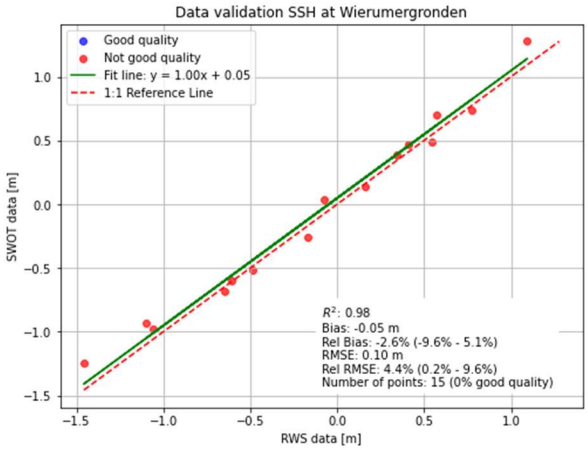
Data validation SSH at Wierumergronden
Good quality
Not good quality
Fit line: y = 1.00x + 0.05
1:1 Reference Line
R^2: 0.98
Bias: -0.05 m
Rel Bias: -2.6% (-9.6% - 5.1%)
RMSE: 0.10 m
Rel RMSE: 4.4% (0.2% - 9.6%)
Number of points: 15 (0% good quality)
SWOT data [m]
RWS data [m]

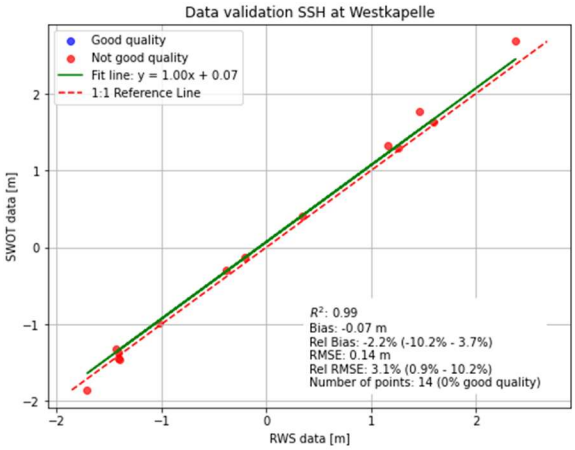
Data validation SSH at Westkapelle
Good quality
Not good quality
Fit line: y = 1.00x + 0.07
1:1 Reference Line
R^2: 0.99
Bias: -0.07 m
Rel Bias: -2.2% (-10.2% - 3.7%)
RMSE: 0.14 m
Rel RMSE: 3.1% (0.9% - 10.2%)
Number of points: 14 (0% good quality)
SWOT data [m]
RWS data [m]

Appendix C: Hourly reconstructions of SSH in the North Sea

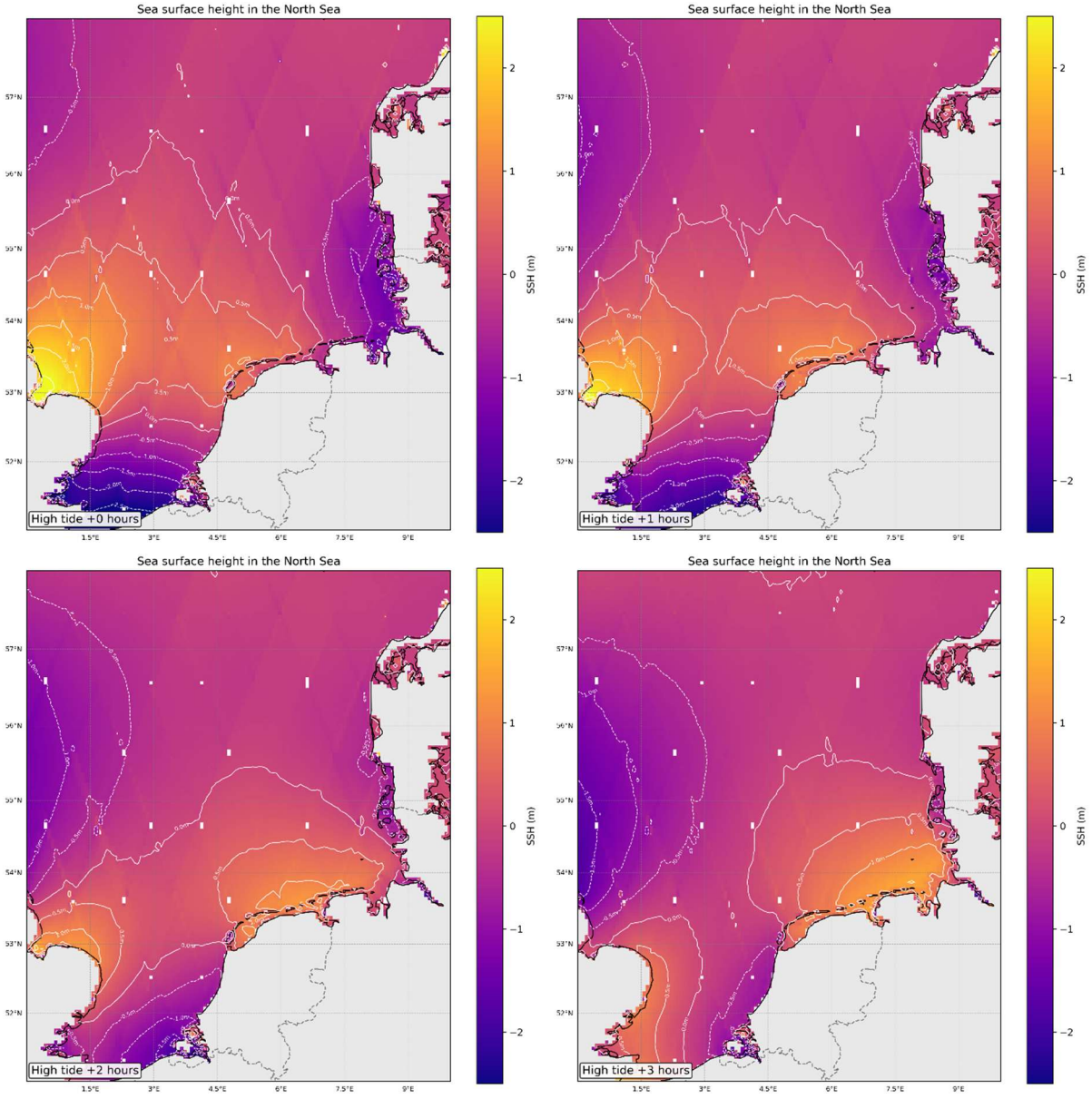

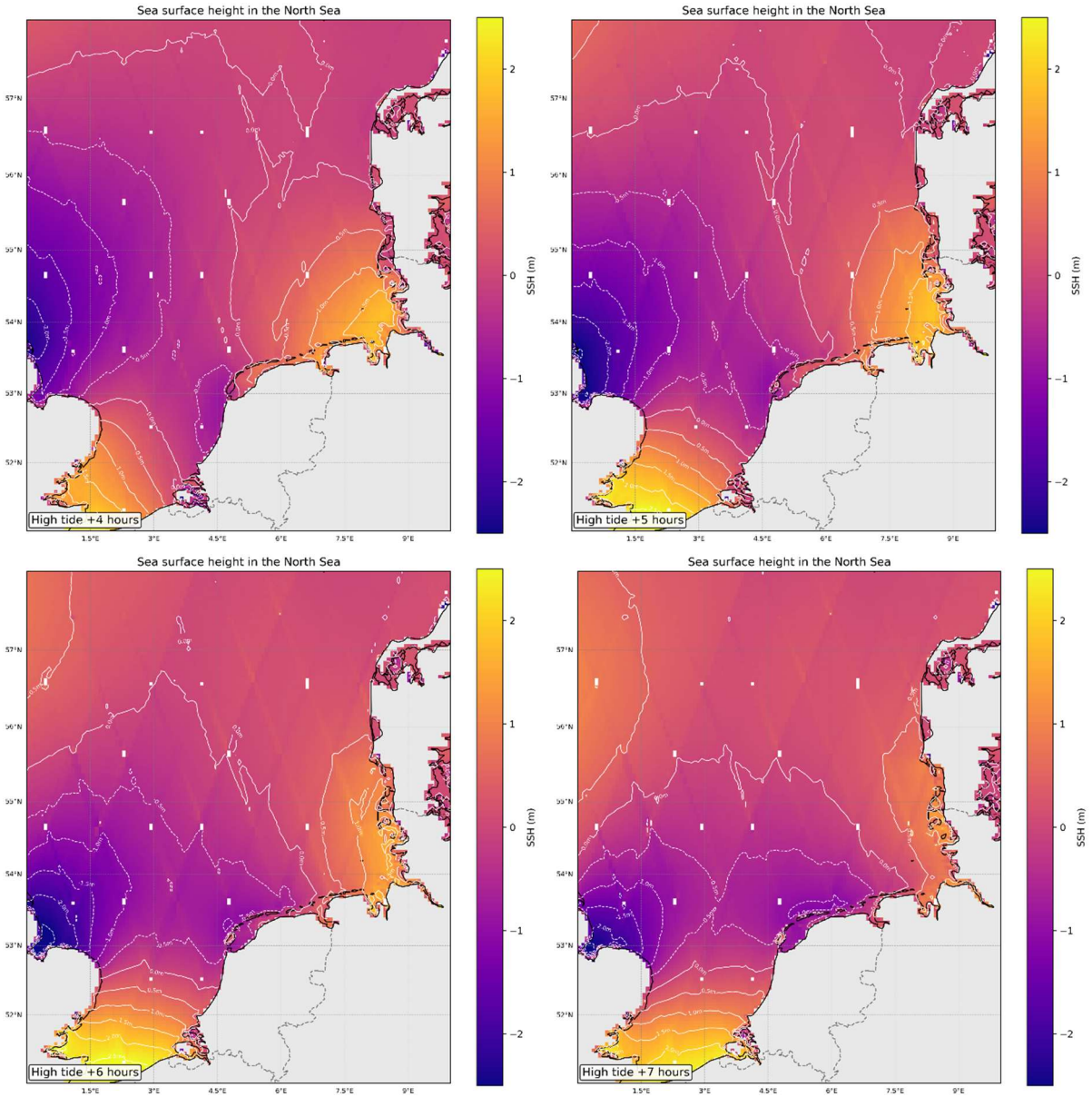
Sea surface height in the North Sea
High tide +4 hours
Sea surface height in the North Sea
High tide +5 hours
Sea surface height in the North Sea
High tide +6 hours
Sea surface height in the North Sea
High tide +7 hours
SSH (m)
57°N
56°N
55°N
54°N
53°N
52°N
1.5°E
3°E
4.5°E
6°E
7.5°E
9°E
2
1
0
−1
−2

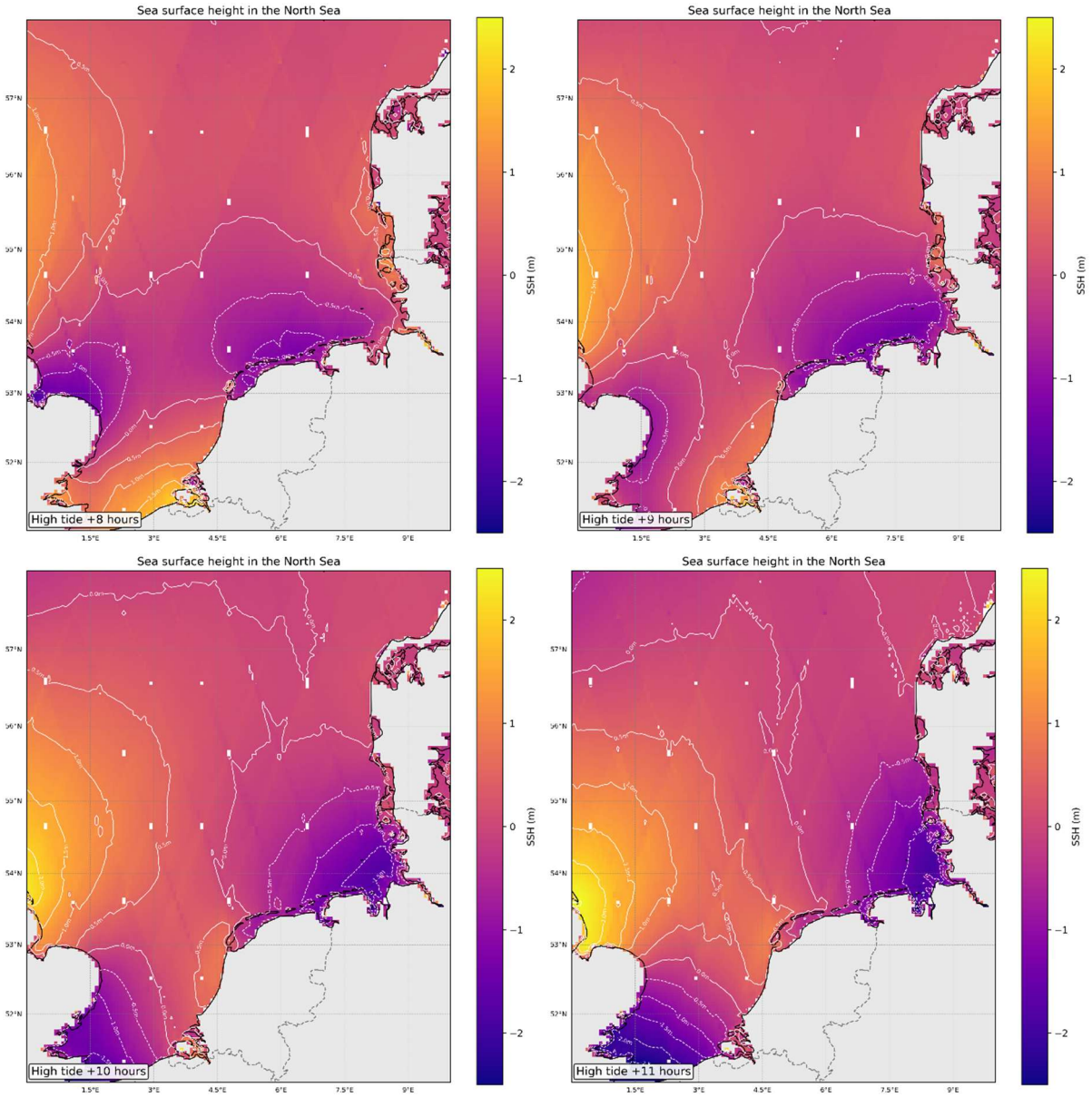
Sea surface height in the North Sea
High tide +8 hours
Sea surface height in the North Sea
High tide +9 hours
Sea surface height in the North Sea
High tide +10 hours
Sea surface height in the North Sea
High tide +11 hours
SSH (m)